ORIGINAL RESEARCH

Identification of the Mtus1 Splice Variant as a Novel Inhibitory Factor Against Cardiac Hypertrophy

Shin Ito, MD; Masanori Asakura, MD, PhD; Yulin Liao, MD, PhD; Kyung-Duk Min, MD, PhD; Ayako Takahashi, MD, PhD; Kazuhiro Shindo, MD; Satoru Yamazaki, PhD; Osamu Tsukamoto, MD, PhD; Hiroshi Asanuma, MD, PhD; Masaki Mogi, MD, PhD; Masatsugu Horiuchi, MD, PhD; Yoshihiro Asano, MD, PhD; Shoji Sanada, MD, PhD; Tetsuo Minamino, MD, PhD; Seiji Takashima, MD, PhD; Naoki Mochizuki, MD, PhD; Masafumi Kitakaze, MD, PhD

***Background*—**In cardiac hypertrophy and failure, there is a widespread alteration in mRNA splicing, but the role of splice variants in cardiac hypertrophy has not yet been fully elucidated. In this study, we used an exon array to identify novel splice variants associated with cardiac hypertrophy.

***Methods and Results*—**We performed genome-wide exon array analysis and developed a splicing profile in murine hearts with hypertrophy induced by transverse aortic constriction for 8 weeks. Following global analysis of splice variants using the Mouse Exon 1.0 ST Array, we identified 46 spliced genes and narrowed our focus to 1 gene, mitochondrial tumor suppressor 1 (*Mtus1*), whose splice variants were registered in the NCBI RefSeq database. Notably, one of the splice variants *Mtus1A* was specifically upregulated, although the total expression of the *Mtus1* gene remained unchanged. We showed that Mtus1A was localized in the mitochondria, and its expression level increased with the degree of cardiac hypertrophy. In cultured cardiomyocytes, Mtus1A overexpression reduced phenylephrine-induced reactive oxygen species production and consequent ERK phosphorylation, resulting in a decrease in both cell size and protein synthesis. In vivo, cardiac-specific Mtus1A transgenic mice showed left ventricle wall thinning and a reduced hypertrophic response to pressure overload and phenylephrine treatment.

***Conclusions*—**We found that *Mtus1* is specifically spliced in hypertrophic hearts and that the Mtus1A variant has an inhibitory effect on cardiac hypertrophy. Mtus1A is, therefore, a possible diagnostic and therapeutic target for cardiac hypertrophy and failure. **(*J Am Heart Assoc*. 2016;5:e003521 doi: 10.1161/JAHA.116.003521)**

Key Words: cardiac hypertrophy • gene array • gene expression/regulation • molecular biology • splice variant

Cardiac hypertrophy is an intervening phenomenon that may predispose the heart to cardiac failure. Using molecular biological techniques, many researchers have identified the genes and proteins involved in the pathophysiology of cardiac hypertrophy.[1–6] Particularly, 3′ in vitro translation microarray technology has been widely used to examine the expression levels of thousands of genes simultaneously.[7–9] However, a conventional 3′ in vitro translation microarray, in which the probes are designated to be near the 3′ end of each gene, is inadequate for investigating genes encoding multiple splice variants, whereas an exon array, by providing probe sets in all exons, is capable of detecting all transcripts.[10] Splicing analysis may, therefore, provide additional information regarding the pathophysiology of cardiac hypertrophy.

Approximately 74% to 95% of human genes undergo multiple alternative splicing events,[11,12] more than half of which are regulated in a cell-type-specific, tissue-specific, or

From the Departments of Cell Biology (S.I., K.-D.M., A.T., K.S., S.Y., N.M.) and Clinical Research and Development (M.A., M.K.), National Cerebral and Cardiovascular Center, Osaka, Japan; Department of Cardiology, Nanfang Hospital, Southern Medical University, Guangzhou, China (Y.L.); Department of Cardiovascular Medicine, Kyoto Prefectural University of Medicine, Kyoto, Japan (H.A.); Department of Molecular Cardiovascular Biology and Pharmacology, Graduate School of Medicine, Ehime University, Ehime, Japan (M.M., M.H.); Departments of Medical Biochemistry (O.T., S.T.) and Cardiovascular Medicine (Y.A., S.S., T.M.), Osaka University Graduate School of Medicine, Osaka, Japan.

Accompanying Tables S1 through S3, Figures S1 through S7, and Videos S1 through S4 are available at http://jaha.ahajournals.org/content/5/7/e003521.full#sec-43

Correspondence to: Masanori Asakura, MD, PhD, Department of Clinical Research and Development, National Cerebral and Cardiovascular Center, 5-7-1 Fujishirodai, Suita, Osaka 565-8565, Japan. E-mail: masakura@ncvc.go.jp

Received March 15, 2016; accepted May 24, 2016.

developmental manner.[13] A genome-wide study has shown widespread alteration in mRNA splicing in the hearts of patients with heart failure, indicating its involvement in the pathogenesis of cardiac diseases.[14–16] We performed a global analysis of splice variants in murine hypertrophic hearts using an exon array and identified the mitochondrial tumor suppressor 1 (*Mtus1*) splice variant associated with cardiac hypertrophy. The *Mtus1* gene was first reported as a tumor suppressor gene localized in the mitochondria,[17] and 3 splice variants of the *Mtus1* gene have since been reported in mice.[18] Several studies revealed that the Mtus1A variant (corresponding to ATBP50) suppresses ERK phosphorylation, which leads to the inhibition of cell proliferation.[18–20] It is well established that the ERK pathway plays an essential role in the signaling of cardiac hypertrophy.[6] These findings led us to investigate the role of the Mtus1A variant during cardiac hypertrophy progression. Our findings provide the first evidence that Mtus1A has an inhibitory effect on cardiac hypertrophy.

Methods

Antibodies and Reagents

Phenylephrine (PE; 046K1351), angiotensin II (Ang II; A9525), and anti-FLAG M2 monoclonal antibody (A8592, F1804) were purchased from Sigma–Aldrich (St. Louis, MO). Antibodies against Actin (sc-1615) and donkey anti-goat IgG (sc-2020) were purchased from Santa Cruz Biotechnology (Santa Cruz, CA) for Western blotting. Antibodies against phospho-ERK1/2 (#9101S), phospho-MEK (#9121S), MEK (#9122S), p-c-Raf (#9427S), c-Raf (#9422), Histone H3 (#9715), α-tubulin (#2144), and rabbit IgG (#7074S) were purchased from Cell Signaling Technology (Danvers, MA). The antibody against ERK1/2 (V114A) was purchased from Promega (Madison, WI). The antibody against Tom20 (612278) was purchased from BD Biosciences (San Jose, CA). The antibody against glyceraldehyde3-phosphate dehydrogenase (Gapdh) (HAB374) was purchased from EMD Millipore (Billerica, MA). The antibody against α1 Na, K-ATPase (ab7671) was purchased from Abcam (Cambridge, UK). An anti-Mtus1 polyclonal antibody raised in rabbits targeted a peptide (CSPKRSPTSSAIPFQSPRNSGSFSSP-SISPR) within the C terminus of the protein. The antibodies for immunofluorescence staining of Alexa mouse Fluor 488 (A11029), rabbit Fluor 488 (A11034), rabbit Fluor 546 (A11035), Fluor 568 phalloidin (A12380), and 4′,6-diamidino-2-phenylindole (DAPI) (D1306) were purchased from Invitrogen (Carlsbad, CA).

RNA Isolation and Array Hybridization

Total RNA from myocardial samples was purified using RNeasy MinElute columns (Qiagen, Hilden, Germany). High RNA quality was confirmed in all samples using an Agilent 2100 Bioanalyzer (Agilent Technologies, Santa Clara, CA). One microgram of total RNA was labeled using the Whole Transcript Sense Target Labeling Assay (Affymetrix, Santa Clara, CA) and hybridized to Mouse Exon 1.0 ST Arrays (Affymetrix) overnight before scanning using an Affymetrix GCS 3000 7G scanner.

Exon Array Analysis

Exon array CEL files were loaded into ArrayAssist software (Stratagene Software Solutions). Probe sets at the core level were summarized using the ExonPLIER algorithm and normalized with antigenomic background probes. For valiance stabilization, the value of 16 was added to the probe set intensity values before transformation to a $\log_2$ scale. Quality analysis confirmed that the data were suitable for assessment. Background noise was detected according to the detection above background algorithm, and probe set signals below the background noise level were filtered out. Probe set level analysis was performed using the ExonPLIER algorithm. Gene expression level analysis was performed using TranscriptPLIER. A splicing index, defined as $\log_2$ (individual exon signal/gene expression level signal), was calculated for all probe sets. If the difference in splicing index between sham and hypertrophic hearts was greater than 1.0 (indicating a fold change $\geq$2) and statistically significant ($P<0.05$), the exon was considered to have been spliced in or out during cardiac hypertrophy. Genes with more than 2-fold changes in expression level ($P<0.05$) were excluded from this study. For efficient functioning of the alternative splicing algorithms, genes with a low expression level (transcription signal <5) in hearts were excluded from the analysis. Finally, the selected genes were inspected in the University of California Santa Cruz (UCSC) genome browser to localize and describe alternative splicing events.

RNA-Seq Library Preparation and Sequencing

Total RNA samples of 2.5 μg each were prepared for RNA-Seq using the Illumina TruSeq RNA Sample Prep Kit v2 (Illumina, San Diego, CA), following the manufacturer's instructions. We assessed the size and purity of cDNA libraries using an Agilent 2100 Bioanalyzer (DNA 1000 kit) and qualified the libraries by quantitative polymerase chain reaction (PCR) using a KAPA library quantification kit (NIPPON Genetics Co, Tokyo, Japan). After denaturation, 15 pmol/L of the libraries was sequenced on an Illumina MiSeq utilizing 75-bp paired-end reads. The sequence data were analyzed using CLC Genomics Workbench (CLC Bio, Aarhus, Denmark). The sequenced reads were mapped to the reference mouse genome (MGSCv37).

Experimental Animal Models

Generation of mice with transverse aortic constriction (TAC)

We subjected C57BL/6J male mice (age, 8 weeks) to TAC or sham operation and measured their hemodynamic parameters as previously reported.[21] Echocardiography was performed using a Vevo 2100 ultrasound system (VisualSonics Inc, Toronto, Canada) equipped with a 30-MHz transducer.

Pharmacologically induced cardiac hypertrophy models

C57BL/6J male mice (age, 6 weeks) were infused with PE (75 mg/kg per day), Ang II (1000 ng/kg per minute), or saline using mini-osmotic pumps (Alzet, Cupertino, CA) to induce cardiac hypertrophy. After the hemodynamic parameters were measured, the PE-treated mice were euthanized 7 days after pump implantation, and the Ang II-treated mice at 14 or 28 days.

All experiments were conducted in accordance with the National Institutes of Health Guide for the Care and Use of Laboratory Animals, and were approved by the ethical committee of Osaka University and National Cerebral and Cardiovascular Center.

Subcellular Fractionation

Murine hearts were pulverized under liquid nitrogen and homogenized at 4°C in homogenate buffer (0.25 mol/L sucrose, 20 mmol/L HEPES, 1 mmol/L EDTA, pH 7.4, including a protease inhibitor cocktail). The nuclear fraction of the homogenate was pelleted by centrifugation at 700*g* for 10 minutes at 4°C. The postnuclear supernatant was further centrifuged at 1000*g* for 10 minutes at 4°C and the pellet was discarded. The cytosolic fraction was obtained by ultracentrifugation at 120 000*g* for 1 hour at 4°C. The supernatant was added to 2 mL of each solution (10%, 15%, 20%, 25%, 30%, and 40%), using OptiPrep™ density gradient solution (Sigma). The solutions were then ultracentrifuged at 107 000 *g* for 13 hours at 4°C using a SW41 Ti swing bucket rotor (Beckman Coulter, CA). After that we were able to obtain the plasma membrane and mitochondrial fractions.

Cell Culture and Treatment

Primary cultures of cardiomyocytes were prepared from the ventricles of 1-day-old Wistar rats, as reported previously.[22] After separation from cardiac fibroblasts, the cardiomyocytes were plated at 75×10^4 cell/mL on collagen-coated culture dishes with DMEM containing 10% FCS. For immunofluorescence staining, cardiomyocytes were plated at 20×10^4 cell/mL on a collagen-coated 4-well Lab-Tek™ chamber slide. For analysis of the cell surface area, the cells were cultured with DMEM containing 1% FCS 48 hours after plating. After 24-hour incubation with 1% FCS, 100 μmol/L PE was added to the medium, and the cells were stimulated for 48 hours. To evaluate protein phosphorylation, the cells were starved in serum-free DMEM after washing (3 times) with phosphate-buffered saline. Following starvation for 24 hours, 10 μmol/L PE was added to the medium, and the cells were stimulated for 5 minutes. Low-passage cardiac fibroblasts were used (passage 3).

Small Interfering RNA (siRNA) Design and Transfection

Duplexed RNA oligonucleotides (Stealth RNAi) and RNAi with Alexa Fluor 488 were synthesized by Invitrogen. Three types of Stealth RNAi oligonucleotides were tested for their ability to knockdown endogenous Mtus1.

The sequences of siRNAs are as follows (sense strands): Mtus1A-36, 5′-UCACGUCCGCCUAACCGCCAAGGGA; Mtus1A-47, 5′-UUUCGAAGCAGUCCCUUGGCGGUUA; and Mtus1A-75, 5′-UUUCCUGAGCCCAGAAGGAAGCCGG.

As a negative control, Stealth RNAi Negative Control Med GC Duplex #2 (46-5372) was purchased from Invitrogen. Six hours after isolating neonatal rat cardiomyocytes, the cells were transfected with siRNAs (20 nmol/L) using Lipofectamine™ RNAiMAX. The proteins were extracted 72 hours after transfection. We selected Mtus1A-75 because this was the most effective siRNA to knockdown both the mRNA and the protein levels of Mtus1A.

Construction of Adenovirus Vectors

Murine *Mtus1A* (NM_001005865) and *Mtus1C* (NM_001005863) were amplified using PCR from a murine heart cDNA library and inserted into pENTR/D-TOPO vectors using Gateway technology (Invitrogen). We also generated N-terminal deletion mutants of the *Mtus1A* variant: Δ17, Δ24, Δ27, and Δ33 AA with C-terminal FLAG tagging. Adenoviral constructs were generated using the ViraPower Adenoviral Expression System (Invitrogen). The supplied pAd/CMV/V5-DEST/lacZ (Invitrogen) was used as a control. Twenty-four hours after plating on dishes, the cardiomyocytes were transfected with each adenoviral vector at a multiplicity of infection of 20. The adenovirus-mediated overexpression of murine Mtus1A was inhibited with siRNAs targeting rat *Mtus1A*. These samples were transfected with the adenoviral vector at a multiplicity of infection of 80 to adjust Mtus1A expression.

The 2A Peptide Expression Vectors

The T2A (*Thosea asigna* virus 2A) sequence was inserted between the sequences encoding Mtus1A (FL, Δ27 AA) and emGFP. The Mtus1A-T2A-emGFP sequences were cloned into pENTR/D-TOPO vectors using Gateway technology

(Invitrogen). Adenovirus constructs were then generated using the ViraPower Adenoviral Expression System (Invitrogen).

T2A sequence: 5′-GAGGGCAGAGGAAGTCTTCTAACATGC GGTGACGTGGAGGAGAATCCCGGCCCT-3′.

Incorporation of [^{3}H]-Leucine

Protein synthesis in cardiomyocytes was evaluated according to the amount of [^{3}H]-leucine incorporated into cells. Following culture for 24 hours with DMEM containing 1% FCS, 1 μCi/mL [^{3}H]-leucine was added to the medium with or without 100 μmol/L PE for a further 48 hours. After washing (2 times) with PBS, the cells were harvested using trypsin and attached to glass filter mats using a microharvester, and radioactivity was measured using a liquid scintillation counter (Wallac β-plate, Turku, Finland).

Real-Time PCR Analysis of mRNA Levels

Total RNA was extracted from the samples using TRIzol reagent (Invitrogen). cDNA was generated by the reverse transcription of 2 μg total RNA using Omniscript RT kit (Qiagen). Real-time PCR was performed with TaqMan technology using a StepOne Real-Time PCR system (Applied Biosystems, Carlsbad, CA). Variant-specific and common TaqMan probes and primers for *Mtus1* were synthesized by Applied Biosystems. TaqMan probes and primers for *Nppa*, eukaryotic 18S rRNA, and *Gapdh* were also purchased from Applied Biosystems. Data were normalized to those of 18S rRNA or *Gapdh*, and relative expression levels were calculated using an arithmetic comparative $2^{-\Delta\Delta Ct}$ method.

TaqMan probes and primers were designed to detect the *Mtus1* exon 15 to 16 boundary (common exon); the *Mtus1A* exon 7 to 8 boundary; the *Mtus1B* exon 4 to 5 boundary; and the *Mtus1C* over 1 to 2 boundary.

Reactive Oxygen Species (ROS) Measurement

Cardiomyocytes were cultured and then transfected with adenovirus vectors (LacZ-2A-emGFP, full-length Mtus1A-2A-emGFP, Δ27-2A-emGFP) or siRNA with Alexa Fluor 488 (si control, si Mtus1A). Following starvation, the cells were incubated with 5 μmol/L MitoSOX Red (Invitrogen, M36008) for 10 minutes in HBSS/Ca/Mg medium (Invitrogen). ROS production in cardiomyocytes was observed following exposure to 10 μmol/L PE in serum-free DMEM without phenol red (Wako, 040-30095).

Western Blot

For total cellular protein extraction, cells were washed with cold PBS and lysed with lysis buffer (1% NP-40, 150 mmol/L NaCl, 20 mmol/L Tris [pH 7.5], 2 mmol/L EDTA, 50 mmol/L NaF and 1 mmol/L Na_3VO_4, including a protease inhibitor cocktail). An equal amount of protein per well was loaded onto 7.5% to 10% SDS-PAGE gels and transferred onto nitrocellulose membranes. The Bio-Rad ChemiDoc XRS system (Bio-Rad Laboratories, Inc, Hercules, CA) was used for chemiluminescence imaging, and the band density was quantified using Bio-Rad Quantity One 1-D Analysis software (Bio-Rad Laboratories).

Immunofluorescence Staining

Neonatal rat cardiomyocytes were incubated with 500 μmol/L of MitoTracker Red (Invitrogen, M-7512) for 30 minutes. The cells were then fixed with 4% paraformaldehyde at room temperature for 10 minutes, washed (twice) using PBS, and permeabilized with 0.2% Triton-X/PBS (room temperature, 10 minutes). After blocking with 10% FCS/PBS buffer for 1 hour at room temperature, the cells were incubated with Mtus1 antibody (1:500), anti-FLAG M2 monoclonal antibody (1:500), and α-tubulin (1:500) for 1 hour at 4°C. The cells were washed twice using PBS, and incubated with the corresponding secondary antibodies for 1 hour at 4°C (Alexa Fluor 488-, Alexa Fluor 546-, and Alexa Fluor 568-conjugated antibodies, 1:500). After washing sufficiently with PBS, the cells were observed using a fluorescence microscope. The following excitation and emission filters were used: GFP, Ex/Em=489/510 nm; MitoTracker Red, Ex/Em=578/598 nm; and MitoSOX Red, Ex/Em=533/574 nm. Images were visualized using an Olympus Power IX-81 inverted fluorescence microscope (Olympus, Tokyo, Japan) or FLUOVIEW FV10i confocal microscope (Olympus). The images obtained using IX-81 and FLUOVIEW FV10i microscopy were analyzed using MetaMorph (MDS Analytical Technologies, Sunnyvale, CA) and FV10-ASW software (Olympus), respectively. The cell surface area was measured using Scion Image (Scion Corporation, Houston, TX).

Immunohistochemical Staining

Heart samples were fixed in 4% paraformaldehyde overnight at 4°C followed by paraffin embedding. Sections were deparaffinized and rehydrated, and antigen retrieval was performed using EDTA (pH 9.0) in a 95°C water bath for 20 minutes. To block endogenous peroxidase activity, the sections were immersed in 3% hydrogen peroxide in methanol for 15 minutes and then incubated overnight with polyclonal Mtus1 antibody (1:500) in ChemMate Antibody Diluent (DakoCytomation, Tokyo, Japan) at 4°C. After rinsing with Tris Buffered Saline with Tween 20, the sections were labeled with horseradish peroxidase–conjugated anti-rabbit IgG for 30 minutes and then visualized with DAB+ (DakoCytomation, Glostrup, Denmark).

The sections were also stained with hematoxylin–eosin for morphological evaluation and Sirius red to evaluate fibrosis. Images were visualized on a BZ-9000 Biorevo all-in-one fluorescence microscope (Keyence Corp, Osaka, Japan), and the cross-sectional area was measured in more than 100 randomly selected cardiomyocytes using BZ-II Analyzer software (Keyence Corp).

Generation of Cardiac-Specific Mtus1A Transgenic Mice

The *Mtus1A* (NM_001005865) transgene was cloned downstream of the murine α-myosin heavy chain (α-MHC) promoter. The purified DNA used in the microinjection was released from the vector backbone. The transgenic founders were produced by pronuclear injection, using standard methods. Mtus1A transgenic (TG) mice were originally derived from the C57BL/6J Jcl background. Line 13 male mice (age, 6 weeks) were used for further study.

Real-Time PCR-Based Copy Number Assay

The genomic DNA (gDNA) was isolated from mouse tail by the standard phenol-chloroform method. The gDNAs were diluted to a concentration of 5 ng/μL and then mixed with 2x TaqMan Genotyping Master Mix and TaqMan primers and probes for *Mtus1* and *Tfrc* (Applied Biosystems). The number of transgene copies was calculated using an arithmetic comparative $2^{-\Delta\Delta Ct}$ method.

Statistical Analysis

This study was designed to examine the inhibitory effects of Mtus1A against cardiac hypertrophy using several parameters for hypertrophy. Statistical analyses were performed to compare the splicing index, the expression of Mtus1, the left ventricular posterior wall thickness (LVPWT), cell size, protein synthesis, ERK activation, and ROS production between controls and intervention groups.

All tests for statistical significance were two-sided. Student *t* test and Mann–Whitney *U* test were used to study differences between groups. All data are expressed as mean±SD.

Results

Global Analysis of Exon Expression Levels in Hypertrophic Hearts

To investigate the role of alternative splicing in the pathogenesis of cardiac hypertrophy leading to heart failure, we induced cardiac hypertrophy by TAC for 8 weeks (Table S1). We performed global analysis of exon and gene levels in these hearts, using the Mouse Exon 1.0 ST Array. Of the 222 710 probe sets mapped on 17 705 genes, we filtered out those with signal levels below the background noise level, leaving 161 159 probe sets for 10 766 genes (Figure 1A). In 3677 (2.28%) of these remaining probe sets, the exon level changed in the TAC hearts to more than double the level in the control hearts. We selected 756 genes that contained at least 1 of these 3677 probe sets and then separately performed splicing and gene-level analysis. Subsequently, to normalize and quantify the exon expression level, we calculated the splicing index, enabling us to compare the splicing analysis between the 2 groups.[10]

We classified these 756 genes into 4 groups according to whether the observed changes in the gene expression level and/or the splicing pattern were greater than 2-fold, with $P<0.05$. We identified 113 genes with significant changes in the splicing pattern but not in the expression level; 112 genes with changes in the expression level but not in the splicing pattern; 140 genes with changes in both the expression level and splicing pattern; and 391 genes without changes in the expression level and splicing pattern (Figure S1).

Identification of *Mtus1* as a Spliced Gene in Hypertrophic Hearts

In this study, we focused on the spliced genes that are incapable of being detected using 3′ in vitro translation microarray. Thus, we narrowed our investigation to the 113 genes with significant changes in the splicing pattern but no change in the gene expression levels when comparing the TAC and control hearts. We then excluded 67 genes with a low expression level in both the control and TAC hearts, leaving 46 candidate genes (Table S2).

Eventually, we focused on the *Mtus1* gene, the only gene whose splice variants were registered in the NCBI RefSeq database (Figure 1A). The *Mtus1* gene is located on chromosome 8 and contains 16 exons. The *Mtus1* gene encodes 3 splice variants that differ in the 5′ exon: *Mtus1A* (NM_001005865) utilizes exons 7 to 16; *Mtus1B* (NM_001005864) utilizes exons 4 to 16, lacking exon 7; and *Mtus1C* (NM_001005863) utilizes exons 1 to 16, lacking exons 4 and 7 (Figure 1B). The exon array indicated significant differences in the splicing indices mapped on exons 2 to 7. The splicing indices mapped on exons 2 to 6 were downregulated in TAC hearts, whereas the splicing index mapped on exon 7 was upregulated. The splicing indices mapped on exons 8 to 16 were unchanged (Figure 1B). These results indicate that *Mtus1A* is upregulated; but both *Mtus1B* and *Mtus1C* are downregulated in hypertrophic hearts. The RNA-Seq read coverage of each exon was similar to the exon array data and showed no other *Mtus1* variants existed (Figure S2).

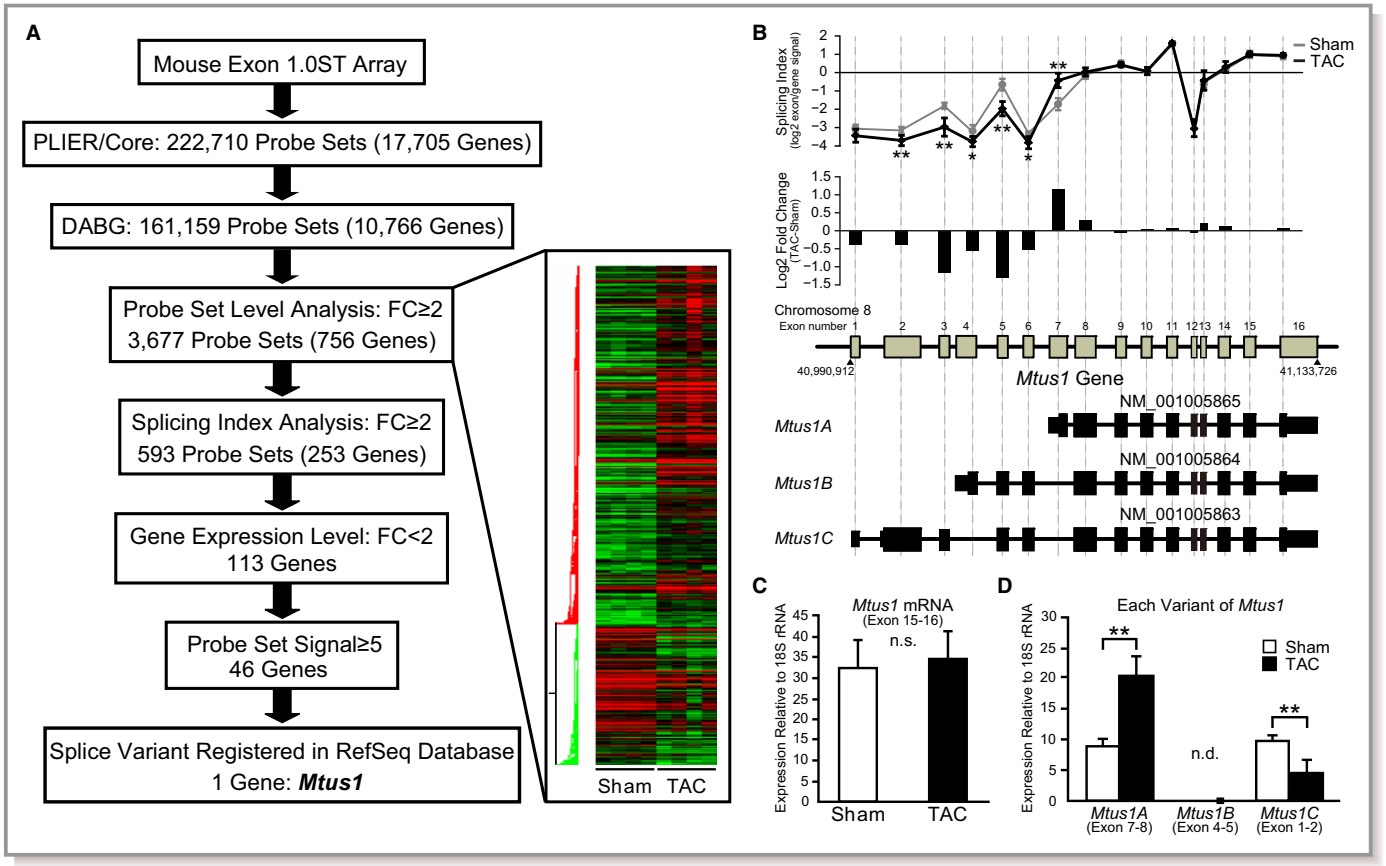

Figure 1. Exon array analysis for the identification of spliced genes in hypertrophic hearts. A, Sham-operated and pressure-overloaded hearts (each n=4) induced by transverse aortic constriction (TAC) for 8 weeks were analyzed using the Mouse Exon 1.0 ST Array. Following the application of the algorithm (left), we performed global analysis of the exon array using ArrayAssist. The right-hand figure shows the hierarchical clustering of 3677 probe sets that were significantly altered in the pressure-overloaded hearts (fold change [FC] ≥2; $P<0.05$). Red and green boxes indicate high and low expressions of the probe sets, respectively. B, The line graph shows the results of the splicing indices of mitochondrial tumor suppressor 1 (*Mtus1*), and the bar graph shows the difference in the splicing indices between TAC and sham. *$P<0.05$, **$P<0.01$ vs sham (n=4 in each group). The lower schema represents the alternative splice variants of *Mtus1,* registered in the NCBI RefSeq database; exons and introns are indicated by boxes and lines, respectively. C and D, Real-time polymerase chain reaction validation of *Mtus1* expression. TaqMan probes and primers for detecting *Mtus1* mRNA were designed at the common exon–exon boundaries (exons 15–16). For detecting each variant, primers were designed at the variant-specific exon–exon boundaries (*Mtus1A*; exons 7–8, *Mtus1B*; exons 4–5, *Mtus1C*; exons 1–2). **$P<0.01$ vs sham (n=4 in each group). DABG algorithm indicates detection above the background algorithm; n.d., not detected; n.s., not significant; PLIER, probe logarithmic intensity error.

Validation of *Mtus1* Splice Variant Expression Using Real-Time PCR

Real-time PCR showed no difference between the control and TAC hearts in the gene expression level of *Mtus1* (Figure 1C). In contrast, we observed a significant increase in the expression level of *Mtus1A* mRNA and a significant decrease in the level of *Mtus1C* mRNA in the TAC hearts (Figure 1D). The results from real-time PCR analysis were in accordance with the exon array data. *Mtus1B* was not detected in the hearts.

Mtus1A Protein Level Increased in the Hypertrophic Hearts

To investigate the levels of both Mtus1A and Mtus1C proteins, we generated a Mtus1A polyclonal antibody that recognizes an epitope in the C-terminal region and can detect all Mtus1 variants. We detected the Mtus1A protein as 2 bands between 40 and 50 kDa and detected Mtus1C as a 180-kDa band on Western blots. The Mtus1A and Mtus1C protein levels were significantly increased and decreased, respectively, in the TAC hearts (Figure 2A and 2B). Next, we examined the tissue distribution pattern of each *Mtus1* variant using real-time PCR and observed a high expression level of *Mtus1A* mRNA in the heart, lung, and brain; tissue-specific expression of *Mtus1B* mRNA in the brain; and ubiquitous expression of *Mtus1C* mRNA (Figure S3). To determine the heart cells in which Mtus1 was highly expressed, we detected Mtus1 protein expression in the sham-operated and TAC hearts using immunohistochemical staining. The Mtus1 protein was observed in the myocardial cells but not in the fibrotic lesions (Figure 2C). We also

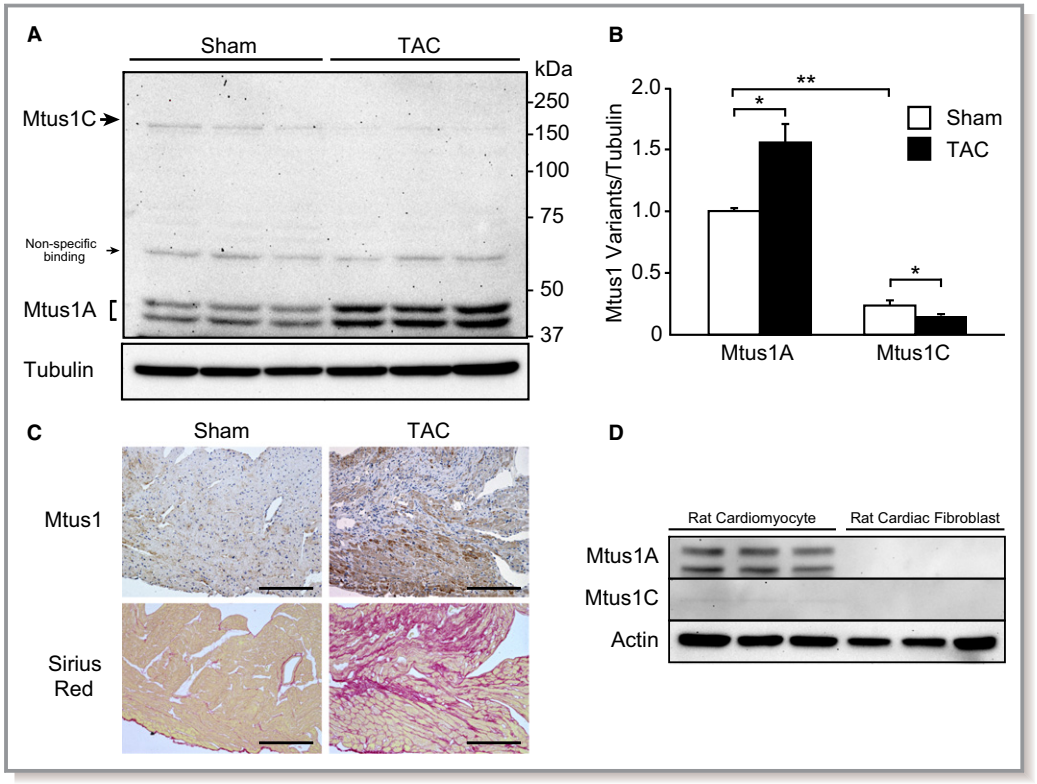

Figure 2. Mitochondrial tumor suppressor 1 (Mtus1) A is upregulated in hypertrophic hearts and predominantly expressed in mitochondria. A, Western blots of Mtus1 variants in murine hearts at 8 weeks after a sham or transverse aortic constriction (TAC) operation (each n=3). An Mtus1 antibody was designed to recognize a peptide within the C terminus of Mtus1 and to detect both Mtus1A and Mtus1C variants. B, Quantitative densitometry of Mtus1 variants relative to α-tubulin. *P<0.05, **P<0.01 vs sham, or as indicated (n=3 sham, n=3 TAC). C, Representative immunohistochemical staining of Mtus1 and Sirius red in murine hearts at 8 weeks after sham or TAC operation (scale bar: 200 μm). D, Western blots of endogenously expressed Mtus1 variants in neonatal rat cardiomyocytes and cardiac fibroblasts.

confirmed that the Mtus1A protein was expressed only in cardiomyocytes and not in cardiac fibroblasts from neonatal rat hearts (Figure 2D). The expression level of the Mtus1C protein was significantly lower than that of Mtus1A (Figure 2B). This result suggested an important role for Mtus1A in the heart and led us to focus our investigation on the Mtus1A variant.

An Association Between Cardiac Hypertrophy and *Mtus1A* Expression

To investigate the association between cardiac hypertrophy and *Mtus1A* expression, we examined the expression levels of myocardial *Mtus1A* in mice at 1, 4, and 8 weeks following TAC. We were able to obtain hypertrophy models with and without heart failure by TAC induction for 8 weeks. We defined heart failure as both the presence of lung edema and reduced ejection fraction. Compared with sham-operated groups at the corresponding weeks, *Mtus1A* expression gradually increased in a time-dependent manner, and the level increased as the LVPWT increased. At 8 weeks, the expression of *Mtus1A* in the hypertrophy models without heart failure significantly increased, compared with the heart failure models (Figure 3A and 3B). These results imply that the *Mtus1A* expression level increases in response to cardiac hypertrophy. We confirmed that the *Mtus1A* expression level was associated with the degree of cardiac hypertrophy in other models induced by Ang II and PE (Figure 3C and 3D).

Mtus1A Is an Inhibitory Factor for Cardiomyocyte Hypertrophy

We found that adenovirus-mediated Mtus1A overexpression suppressed both cell size and protein synthesis in cardiomyocytes (Figure 4 through 4D). In contrast, siRNA knockdown of Mtus1A increased both cell size and protein synthesis in cardiomyocytes (Figure 4E through 4H).

Furthermore, we examined whether the Mtus1A protein inhibited cardiomyocyte hypertrophy induced by PE. Mtus1A overexpression diminished the PE-stimulated increase in both cell size and protein synthesis in cardiomyocytes (Figure 4A through 4D). Conversely, Mtus1A knockdown enhanced PE-induced cardiomyocyte hypertrophy (Figure 4E through 4H).

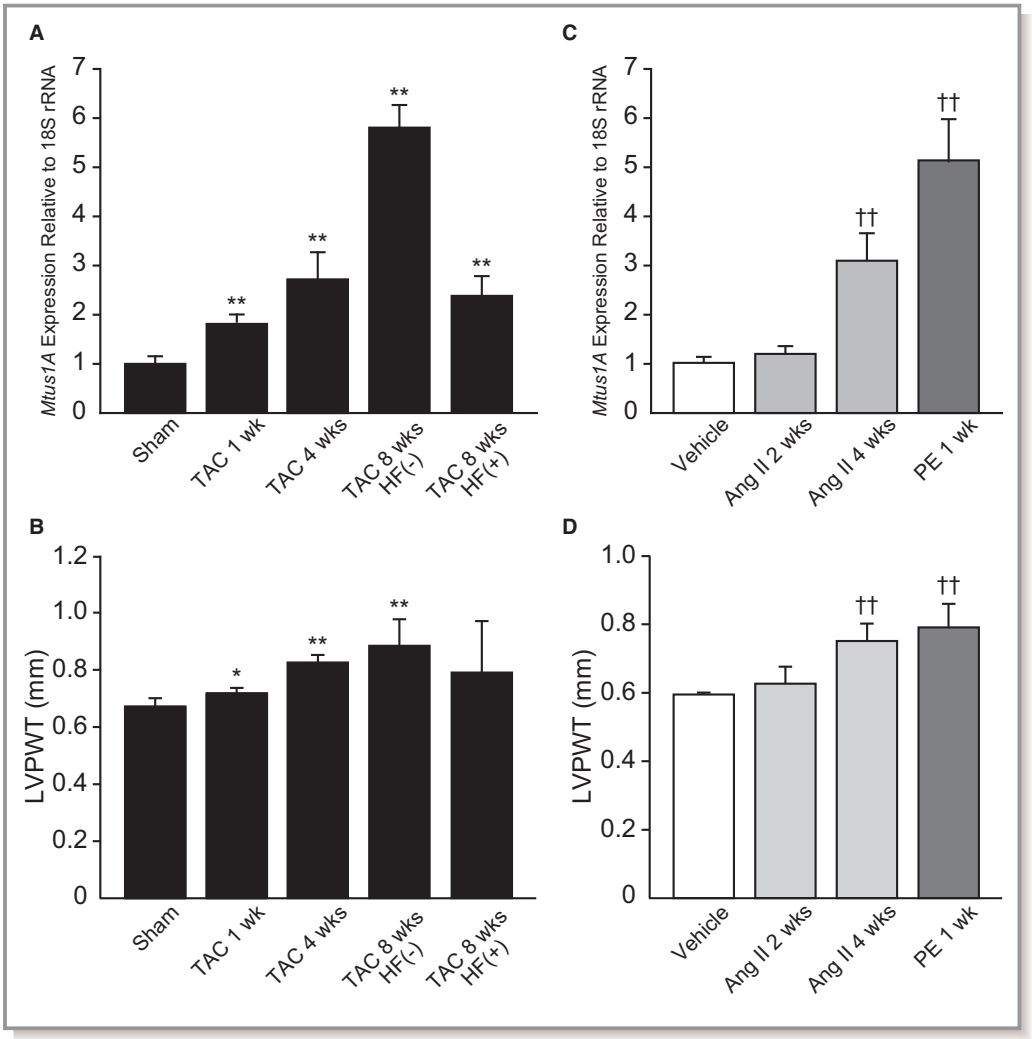

Figure 3. Association between cardiac hypertrophy and mitochondrial tumor suppressor 1 (*Mtus1*) *A* expression. A and B, The *Mtus1A* mRNA expression levels in the myocardium and left ventricular posterior wall thickness (LVPWT) after transverse aortic constriction (TAC), respectively. C57BL/6J mice were subjected to sham for 1, 4, and 8 weeks (n=4 in each group), or TAC operation for 1 (n=6), 4 (n=3) and 8 weeks (without HF, n=3; with HF, n=4). Heart failure (HF) was defined as the presence of lung edema and reduced fractional shortening in mice after 8 weeks of TAC. **P*<0.05, ***P*<0.01 vs sham at the corresponding weeks. There was no significant difference in the expression of *Mtus1A* and LVPWT among the sham groups. Data shown as sham indicated mice at 8 weeks following sham operation. C and D, The *Mtus1A* mRNA expression levels in the myocardium and LVPWT induced by pharmacological agents in cardiac hypertrophy models. C57BL/6J mice were treated with angiotensin II (Ang II) (1000 ng/kg per minute) or phenylephrine (PE) (75 mg/kg per day) using mini-osmotic pumps. Mice treated with Ang II were euthanized at 2 (n=3) or 4 weeks (n=6), and mice treated with PE were euthanized at 1 week (n=3). Control mice were infused with saline for 1, 2, and 4 weeks (n=4 in each group). ††*P*<0.01 vs vehicle at the corresponding weeks. There was no significant difference in the expression of *Mtus1A* and LVPWT among the vehicle groups. Data shown as vehicle indicated mice 4 weeks following saline infusion. The expression levels of *Mtus1A* were normalized to those of 18S rRNA.

These results indicate that Mtus1A has an inhibitory effect on cardiomyocyte hypertrophy.

Mtus1A Modulates the ERK Signaling Cascade

To confirm the cellular mechanism for the inhibitory effect of Mtus1A on cardiomyocyte hypertrophy, we investigated the ERK signaling cascade responsible for cardiac hypertrophy. Mtus1A overexpression attenuated the PE-induced phosphorylation of c-Raf, MEK, and ERK (Figure 5A). We observed an augmentation of PE-induced phosphorylation of c-Raf, MEK, and ERK, following Mtus1A knockdown with siRNA (Figure 5B). Moreover, the enhanced PE-induced activation of ERK signaling following knockdown of Mtus1A

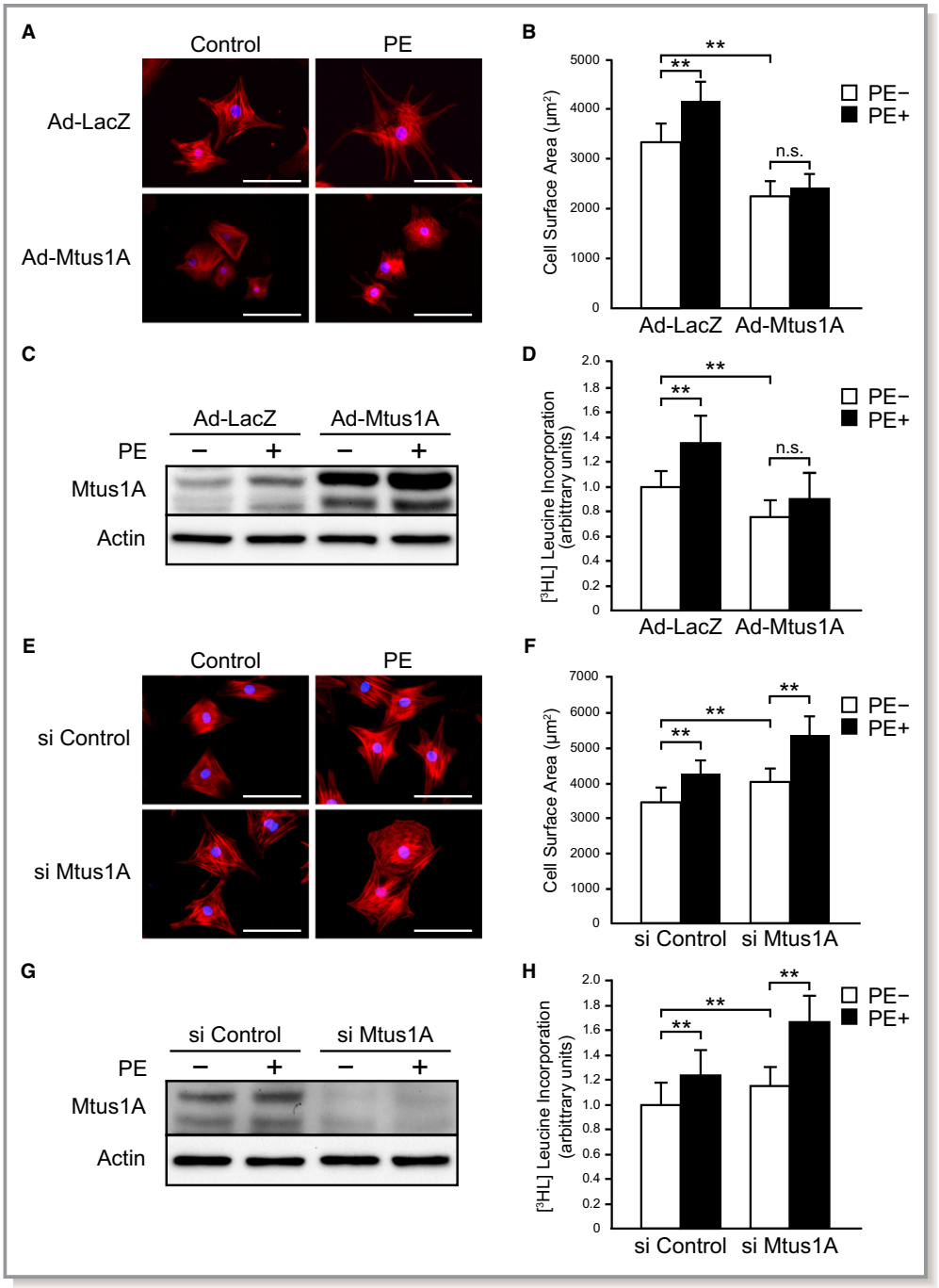

Figure 4. Mitochondrial tumor suppressor 1 (Mtus1) A suppresses cardiomyocyte hypertrophy. A through D, Adenovirus-mediated Mtus1A protein overexpression suppressed cell size and protein synthesis. Cardiomyocytes were infected with Ad-LacZ or Ad-Mtus1A and then cultured in the absence or presence of phenylephrine (PE) (100 μmol/L) for 48 hours. E through H, Mtus1A protein knockdown using small interfering RNA (siRNA) increased cell size and protein synthesis. Cardiomyocytes were transfected with si control or si Mtus1A and then cultured in the absence or presence of PE (100 μmol/L) for 48 hours. A and E, Representative phalloidin staining of cardiomyocytes. Nuclei were stained with 4′,6-diamidino-2-phenylindole (DAPI) (blue). Images were visualized using an Olympus IX-81 inverted microscope (scale bar: 30 μm). B and F, The surface area of cardiomyocytes. $^{**}P<0.01$ vs each control, or as indicated (n=100–150 cells in each group). C and G, Western blots of Mtus1A and Actin in cardiomyocytes in the absence or presence of PE (100 μmol/L) for 48 hours. D and H, [^{3}H]-leucine incorporation in cardiomyocytes cultured in the absence or presence of PE (100 μmol/L) for 48 hours. $^{**}P<0.01$ vs each control or as indicated (n=30–40 in each group). n.s. indicates not significant.

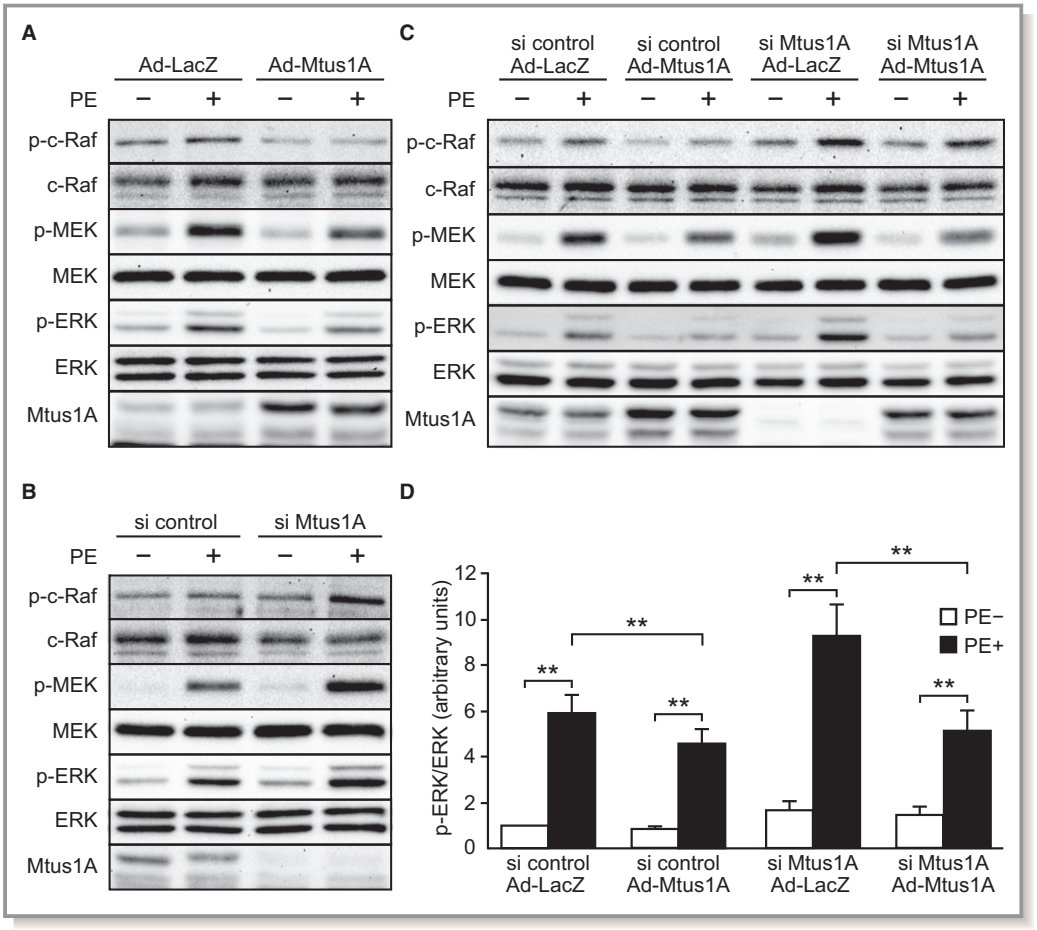

Figure 5. Mitochondrial tumor suppressor 1 (Mtus1) A attenuates ERK phosphorylation. A, Cardiomyocytes were infected with Ad-LacZ or Ad-Mtus1A for 48 hours. B, Cardiomyocytes were transfected with small interfering (si) control or si Mtus1A for 64 hours. C, siRNA-transfected cardiomyocytes were further co-transfected with Ad-LacZ or Ad-Mtus1A. D, Quantitative densitometry of p-ERK relative to total ERK. All samples were starved for 24 hours and treated with 10 μmol/L of phenylephrine (PE) or serum-free medium for 5 minutes. The cell lysates were immunoblotted with antibodies against p-c-Raf, c-Raf, p-MEK, MEK, p-ERK, ERK, and Mtus1. Data are from 5 independent experiments (n=5). $^{**}P<0.01$ vs each control (PE−), or as indicated.

was attenuated by Mtus1A overexpression (Figure 5C and 5D).

Mitochondrial Localization of Mtus1A

We determined the subcellular localization of Mtus1 and detected the Mtus1A protein predominantly in the mitochondria of murine hearts. The Mtus1C protein showed a different expression pattern, as it was expressed in the nucleus and cytosol (Figure 6A and 6B). We next examined the localization of Mtus1 in neonatal rat cardiomyocytes, overexpressing the Mtus1 variants. This confirmed the localization of Mtus1A in mitochondria and Mtus1C in microtubules (Figure S4).

Subsequently, we examined how Mtus1A is targeted to the mitochondria. The protein sequence analysis by MITOPROT II predicted that Mtus1A has a mitochondrial targeting sequence in the exon 1 region. Therefore, we constructed 4 deletion mutants of Mtus1A (Δ17, Δ24, Δ27, and Δ33), designed by targeting arginine residues in exon 1, and overexpressed these mutants using the adenovirus vector (Figure 7A). Full-length (FL), Δ17 and Δ24 Mtus1A mutants were mainly detected in the mitochondria. Δ27 and Δ33 mutants were exclusively detected in the cytosol (Figure 7B). These results clarified that Mtus1A protein is translocated to the mitochondria with a mitochondrial targeting sequence in exon 1.

To examine the nature of 2 distinct bands of Mtus1A in Western blots, we expressed Mtus1A with a C-terminal FLAG tag. We detected 2 bands with the anti-FLAG antibody (Figure S5), and showed that both bands consisted of the Mtus1A protein. The overexpression of Mtus1A with the N-terminus FLAG tag could not be detected as the lower band

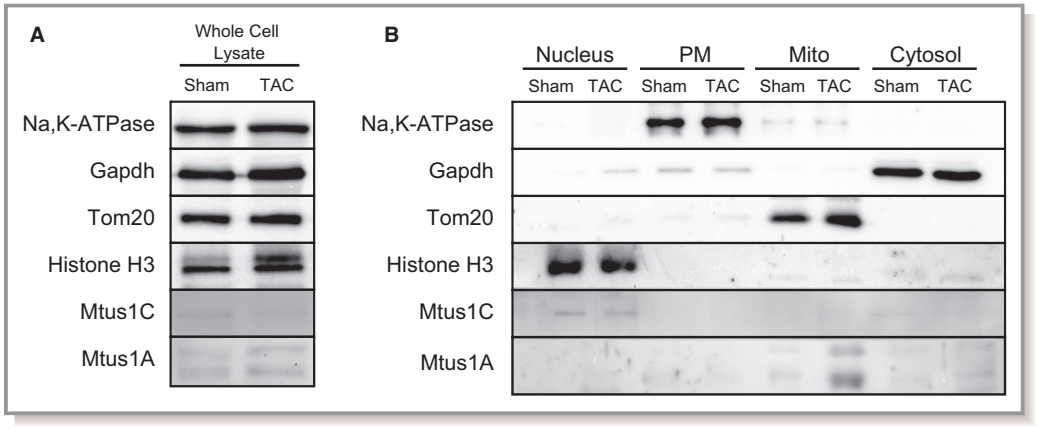

Figure 6. Mitochondrial tumor suppressor 1 (Mtus1) A is localized in mitochondria. A, Western blot analyses in whole cell lysates from murine hearts at 8 weeks after sham or transverse aortic constriction (TAC) operation. B, Western blot analyses in subcellular fractions prepared from murine hearts at 8 weeks after sham or TAC operation. Immunoblot analyses were performed with antibodies against Na, K-ATPase (plasma membrane marker), glyceraldehyde 3-phosphate dehydrogenase (Gapdh) (cytosolic marker), Tom20 (mitochondrial marker), Histone H3 (nuclear marker), and Mtus1. Mito indicates mitochondria; PM, plasma membrane.

and was not localized in the mitochondria (data not shown). The addition of the FLAG tag to the N-terminus of Mtus1A may impair cleavage in the mitochondria, resulting in only the upper band being detected.

Mitochondrial Mtus1A Reduced Cardiomyocyte Hypertrophy

The overexpression of Δ17 and Δ24 Mtus1A mutants suppressed cell size but the overexpression of Δ27 and Δ33 mutants did not (Figure 7C). Moreover, the overexpression of Δ17 and Δ24 Mtus1A mutants attenuated PE-induced phosphorylation of c-Raf, MEK, and ERK (Figure 7D). These results indicate that mitochondrial Mtus1A plays a central role in the regression of cardiomyocyte hypertrophy.

Mtus1A Suppresses Mitochondrial ROS Production

We investigated how Mtus1A modulates ERK signaling in cardiomyocytes. Induction of mitochondrial ROS is known to be 1 of the key factors for the progression of cardiac hypertrophy through the stimulation of Ras/Raf/MEK/ERK signaling.[23,24] We overexpressed Mtus1A protein using 2A peptide expression vectors (Figure S6). Cardiomyocytes overexpressed with Ad-LacZ-2A-emGFP generate significant amounts of ROS after PE treatment. Overexpression of Mtus1A protein in mitochondria, using Ad-FL-Mtus1A-2A-emGFP, reduced PE-induced ROS production. This reduction of ROS production by Mtus1A overexpression in mitochondria was abolished by inhibiting the translocation of Mtus1A to the mitochondria using Ad-Δ27-Mtus1A-2A-emGFP (Figure 8A and 8C). We confirmed that knockdown of Mtus1A in mitochondria enhanced PE-induced ROS production (Figure 8B and 8D). These results implied that Mtus1A inhibits cardiac hypertrophy through the reduction of ERK signaling activated by ROS production.

Cardiac-Specific Overexpression of Mtus1A Inhibits Cardiac Hypertrophy In Vivo

To determine whether Mtus1A regulates cardiac hypertrophy in vivo, we generated TG mice overexpressing *Mtus1A* driven by the α-MHC promoter (Figure 9A). We established the 3 lines of TG mice and observed the upregulation of Mtus1A in their hearts (Figure S7 and Figure 9B). No differences were observed in blood pressure, heart rate, and body weight between the Mtus1A TG and wild-type (WT) mice. However, Mtus1A TG mice showed reductions in the heart-to-body-weight ratio, LVPWT, fractional shortening, and cross-sectional area of cardiomyocytes (Figure 9C, 9D, 9F through 9K and Table S3).

We also investigated whether Mtus1A overexpression in the heart could inhibit cardiac hypertrophy induced by TAC. We observed that TAC-induced increase in LVPWT was reduced and the cell surface area was also suppressed in the Mtus1A TG mice (Figure 9C, 9D, and 9F through 9H). The extent of LV fibrosis after TAC was not significantly different between the TG and WT mice (WT 9.3±0.1% versus TG 8.8±0.8%, P=0.47) (Figure 9E). LV systolic function was significantly impaired in Mtus1A TG mice after TAC (Figure 9F and Videos S1 through S4).

We further investigated whether Mtus1A overexpression inhibits PE-induced cardiac hypertrophy. We observed that the PE-induced increase in LVPWT diminished in the Mtus1A TG mice and that the cell surface area increased to 143% and 111% in the WT and Mtus1A TG mice, respectively (Figure 9I

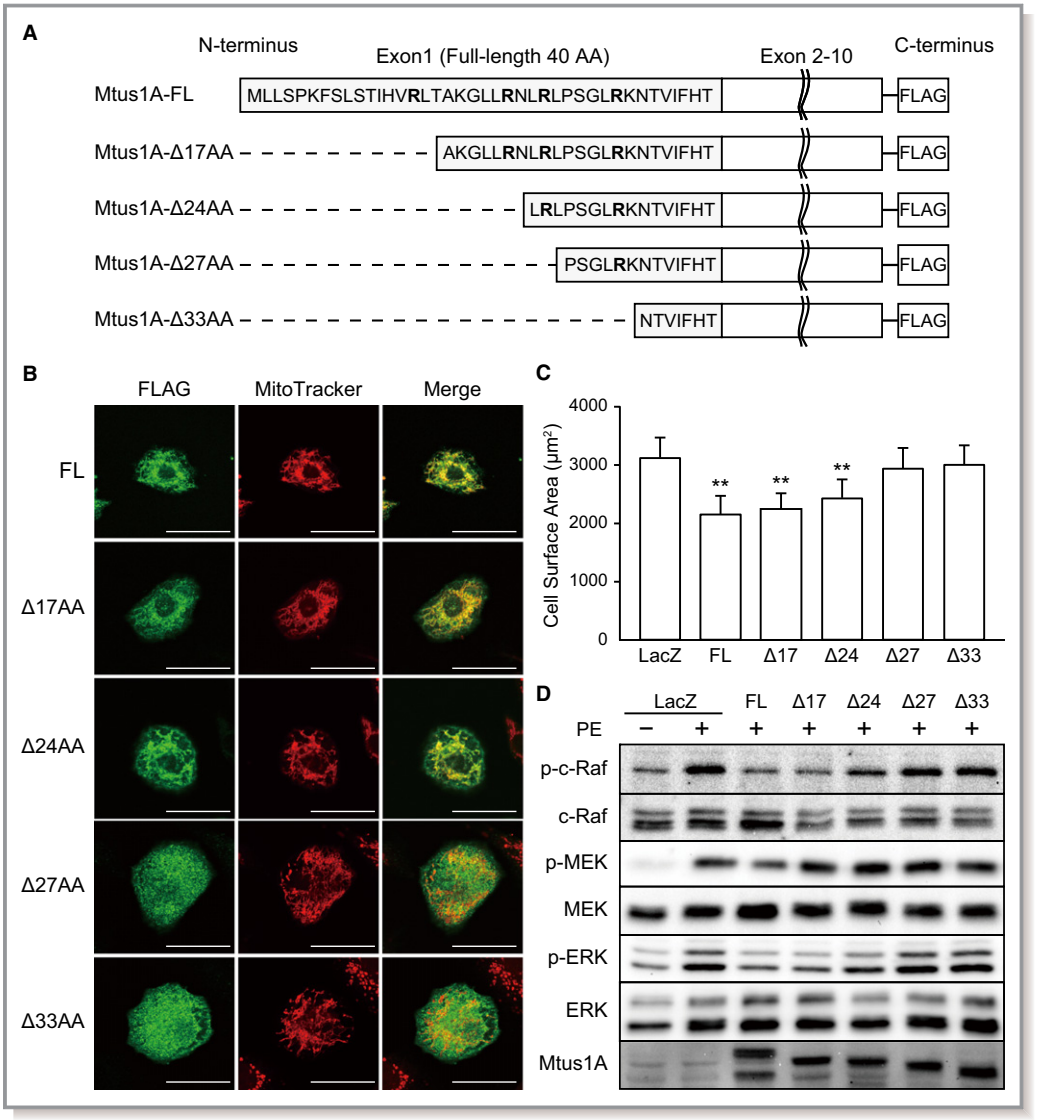

Figure 7. Mitochondrial tumor suppressor 1 (Mtus1) A contains the mitochondrial targeting sequence in exon 1. A, Schematic diagram of Mtus1A deletion constructs. The constructs were designed by targeting arginine residues in exon 1 and tagged with C-terminal FLAG; Full-length (FL), Δ17, Δ24, Δ27 and Δ33. B, Immunofluorescent staining of cardiomyocytes, overexpressing FLAG-tagged deletion mutants of Mtus1A with an adenovirus vector. Mtus1A and mitochondria were stained with anti-FLAG antibody and MitoTracker Red, respectively. In the merged images, the color yellow indicates the co-localization of FLAG-Mtus1A and mitochondria. Images were visualized using FLUOVIEW FV10i confocal microscope (scale bar: 30 μm). C, The surface area of each cardiomyocyte. $^{**}P<0.01$ vs Ad-LacZ (n=50 cells in each group). D, Phosphorylation of c-Raf/MEK/ERK in cardiomyocytes overexpressing deletion mutants of Mtus1A. All samples were starved for 24 hours and treated with 10 μmol/L of phenylephrine (PE) or serum-free medium for 5 minutes. The cell lysates were immunoblotted with antibodies against p-c-Raf, c-Raf, p-MEK, MEK, p-ERK, ERK, and Mtus1.

through 9K). These results indicated that Mtus1A attenuated cardiac hypertrophy.

Discussion

Here global analysis of an exon array identified the Mtus1A variant as a novel regulator of cardiac hypertrophy based on the following evidence: (1) *Mtus1A* expression increased with the extent of cardiac hypertrophy; (2) Mtus1A expressed in the mitochondria reduced PE-induced c-Raf/MEK/ERK phosphorylation, resulting in a decrease in both protein synthesis and the size of cardiomyocytes; (3) Mtus1A suppressed mitochondrial ROS production following PE stimulation in the mitochondria; and (4) cardiac-specific Mtus1A TG mice showed LV wall thinning, LV dysfunction, and reduced hypertrophic response to pressure overload and PE treatment.

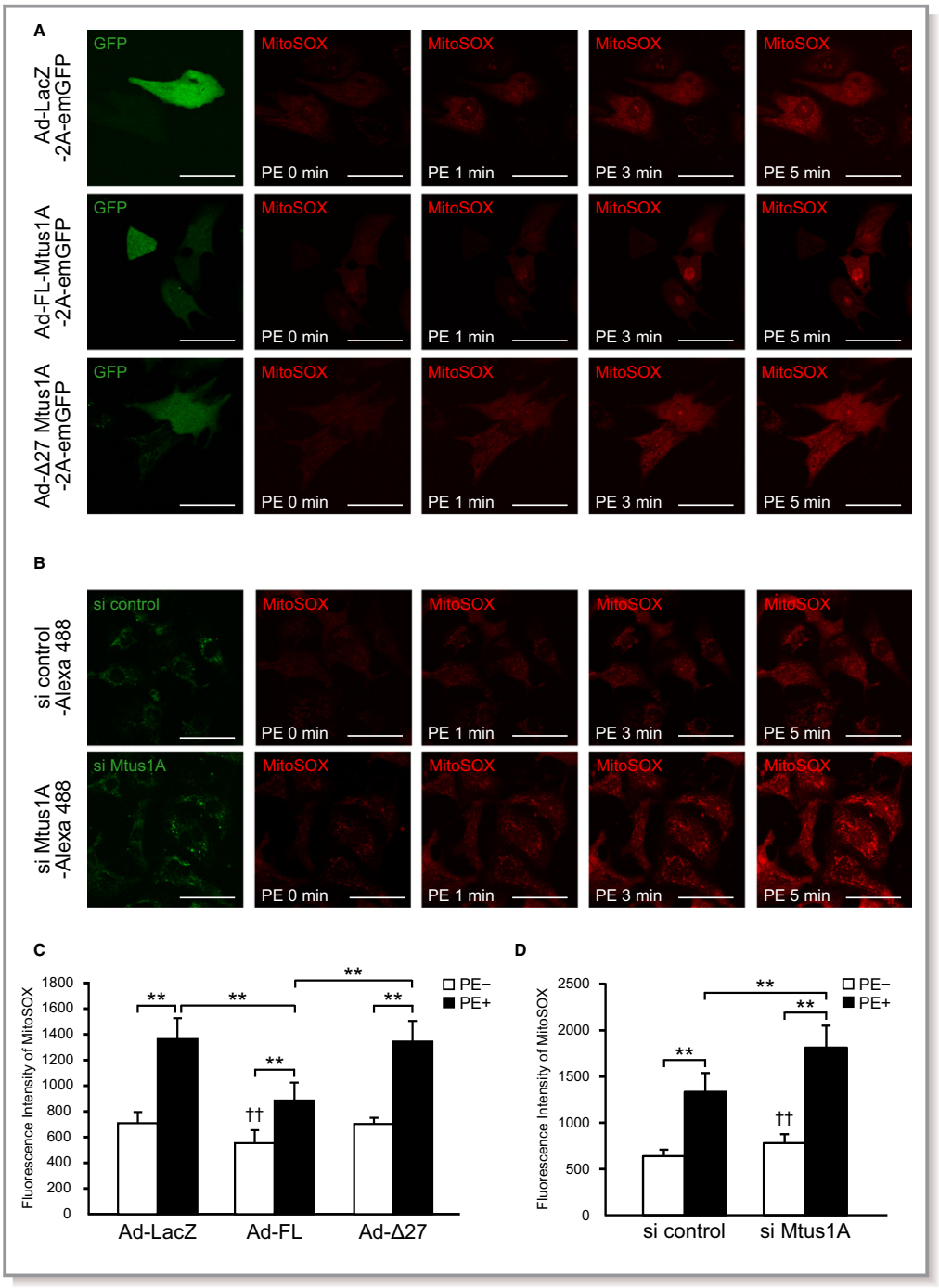

Figure 8. Mitochondrial tumor suppressor 1 (Mtus1) A suppresses mitochondrial reactive oxygen species (ROS) production. A, Real-time detection of mitochondrial ROS production in living cardiomyocytes overexpressing Mtus1A, following stimulation with phenylephrine (PE). Cardiomyocytes were infected with adenoviruses expressing LacZ-2A-emerald green fluorescent protein (emGFP) or Ad-full-length (FL)-Mtus1A-2A-emGFP or Δ27 Mtus1A-2A-emGFP for 48 hours. The cells were starved for 24 hours and stimulated with 10 μmol/L of PE. ROS production was visualized using MitoSOX (red fluorescence) at the indicated time intervals. B, Real-time detection of mitochondrial ROS production after knockdown of Mtus1A in living cardiomyocytes, following stimulation with PE. Cardiomyocytes were transfected with Alexa 488-labeled small interfering (si) control or si Mtus1A for 64 hours. After starvation, ROS production was visualized following stimulation with PE as in (A). C and D, Quantification of ROS production at 5 minutes after stimulation with PE. Fluorescence intensities of ROS within the region of interest were measured (n=50 cells in each group). Images were visualized using a FLUOVIEW FV10i confocal microscope (scale bar: 30 μm). $^{**}P<0.01$ vs each control (PE−), or as indicated; $^{\dagger\dagger}P<0.01$ vs Ad-LacZ without PE or si control without PE.

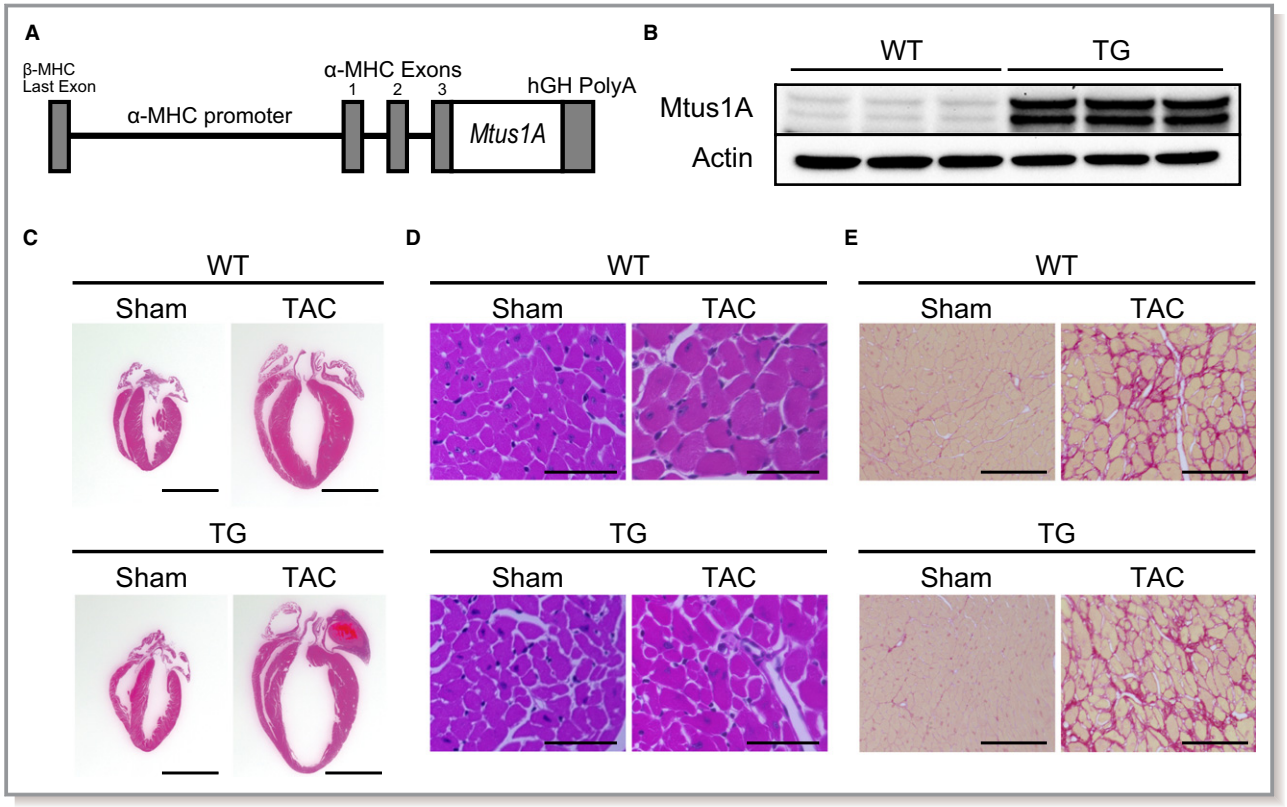

Figure 9. Cardiac-specific mitochondrial tumor suppressor 1 (Mtus1) A overexpression inhibits cardiac hypertrophy in vivo. A, Mouse *Mtus1A* cDNA was fused to the α-myosin heavy chain (α-MHC) promoter for the generation of cardiac-specific transgenic (TG) mice. B, Western blots of Mtus1A in line 13 TG mouse hearts. C through E, Mouse hearts from TG and wild-type (WT) littermates after either a sham or transverse aortic constriction (TAC) operation at 4 weeks were longitudinally sectioned (scale bar: 4 mm), and stained with hematoxylin–eosin and Sirius red (scale bar: 50 μm). F, Representative M-mode echocardiographic images of hearts from the WT and TG mice with sham or TAC after 4 weeks. G, Left ventricular posterior wall thickness (LVPWT) in the WT and TG mice after sham or TAC at 4 weeks. $^{**}P<0.01$ vs each control (sham) or as indicated (n=3 WT-sham, n=6 WT-TAC, n=3 TG-sham, n=4 TG-TAC). H, Quantitative analysis of the surface area of cardiomyocytes in the WT and TG mice after sham or TAC at 4 weeks. $^{**}P<0.01$ vs each control or as indicated (n=100–200 cells in each group). I, Representative M-mode echocardiographic images of hearts from the WT and TG mice treated with saline (vehicle) or phenylephrine (PE) at a concentration of 75 mg/kg per day for 7 days. J, LVPWT in the WT and TG mice after saline (vehicle) or PE treatment. $^{*}P<0.05$ vs each control (vehicle) or as indicated (n=5 in each group). K, Quantitative analysis of the surface area of cardiomyocytes in the WT and TG mice after saline (vehicle) or PE treatment. $^{**}P<0.01$ vs each control or as indicated (n=100–200 cells in each group). EDD indicates end-diastolic dimension; ESD, end-systolic dimension; hGH, human growth hormone; n.s., not significant.

Seibold et al identified *Mtus1* as a tumor suppressor gene localized in the mitochondria.[17] Reduced expression levels of Mtus1 are associated with poor prognosis in human tumors, eg, pancreatic,[17] hepatocellular,[25] and colon tumors.[26] The overexpression of Mtus1A inhibits ERK phosphorylation and tumor cell line proliferation.[20,27] These observations strongly support our finding that Mtus1A attenuates cardiac hypertrophy through ERK signaling reduction.

Mtus1A was also identified as a protein capable of interacting with the C-terminal end of the AT2 receptor (also called AT2 receptor-interacting protein 1, ATIP1), using a yeast 2-hybrid system involving in ERK signaling.[18,19] The AT2 receptor is expressed in the cell membrane; however, the Mtus1A protein is reported to be localized in either the mitochondria[17] or the Golgi apparatus.[18] We also showed that Mtus1A was localized in the mitochondria of neonatal rat cardiomyocytes. Fujita et al demonstrated that pretreatment with the AT2 receptor-selective antagonist PD123319 did not affect ERK phosphorylation in systemic ATIP (Mtus1A) TG mice,[28] suggesting the existence of an AT2 receptor-independent mechanism of Mtus1A that suppresses ERK signaling in cardiac hypertrophy. Mitochondria, where Mtus1A is mainly expressed, are the main source of ROS production.[29] Mitochondrial ROS production is activated by hypertrophic stimuli, such as G protein–coupled receptor agonists and pressure overload,[30–32] and induces cardiac hypertrophy through Ras/Raf/MEK/ERK signaling stimulation.[24] This evidence strongly supports our hypothesis that the inhibitory effect of Mtus1A on cardiac hypertrophy is because of the suppression of ROS production.

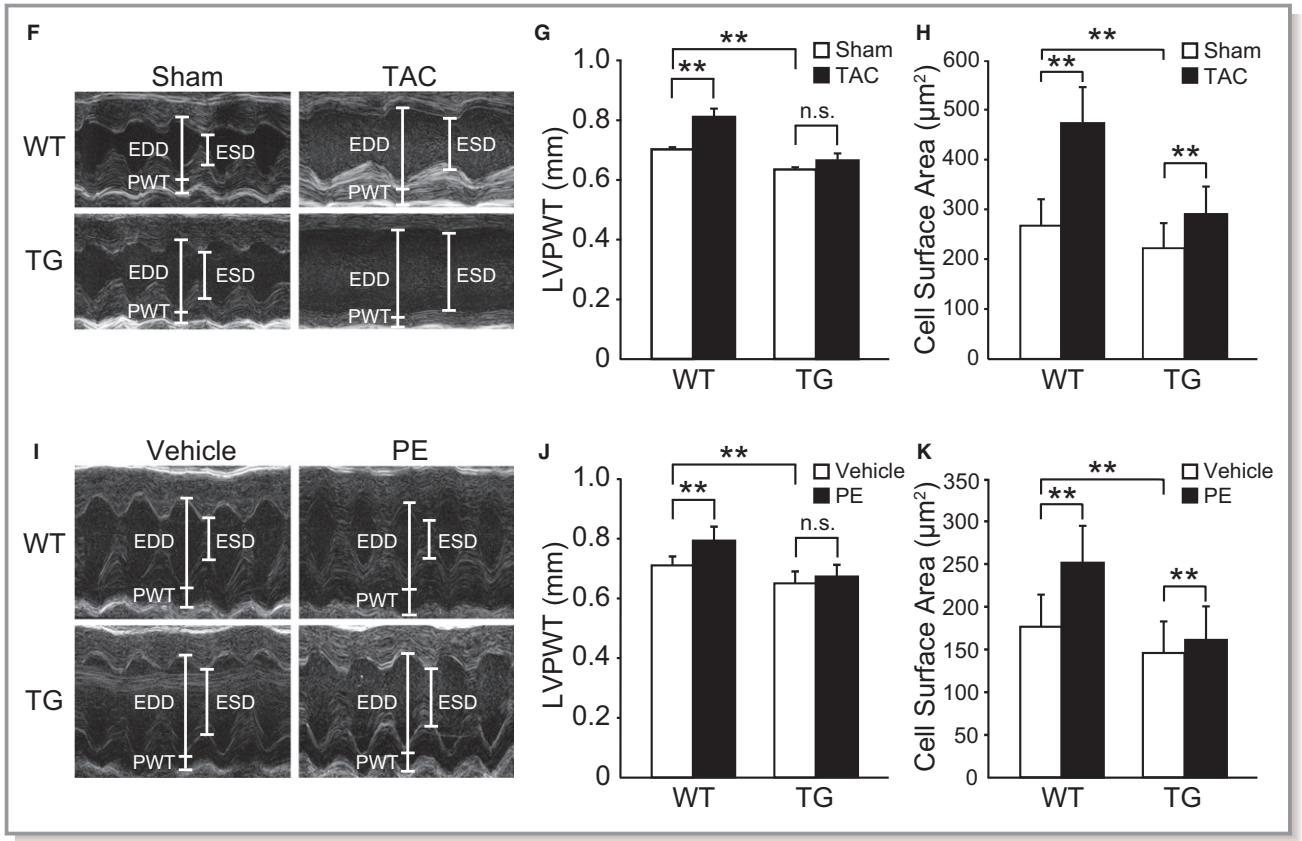

Figure 9. Continued

Cardiac hypertrophy is caused by various stimuli, such as Ang II, PE, isoproterenol, and mechanical stress. These stimuli activate hypertrophic cascades via MEK/ERK, PI3K/Akt, and calcineurin–NFAT cascades, following the activation of transcription factors. MEK/ERK signaling, but not PI3K/Akt signaling, is activated in TAC hearts.[33] MEK protein overexpression in murine hearts induces cardiac hypertrophy.[6] Thus, MEK/ERK signaling is vital in cardiac hypertrophy, and MEK/ERK signaling modulation is a potential therapeutic target for cardiac hypertrophy. Recently, a few molecules, such as Carp and Erbin, have been reported to suppress cardiac hypertrophy through ERK signaling inhibition.[33,34] Song et al reported that Carp overexpression reduced cardiac hypertrophy, but the function of endogenous Carp on cardiac hypertrophy remains unclear.[33] Rachmin et al reported that Erbin expression is reduced in hypertrophic hearts, and Erbin knockout mice exhibited cardiac hypertrophy.[34] Unlike Erbin, we first identified the splice variant induced by cardiac hypertrophy, finding that this variant suppresses ERK signaling activated in a cardiac hypertrophic state.

Recently, Zuern et al revealed that systemic Mtus1 knockout mice, lacking all splice variants, exhibited renal disease, lymphoid hyperplasia, and cardiac hypertrophy.[35] This cardiac phenotype agreed with the present observation; however, because renal diseases are usually associated with cardiac hypertrophy, it is still unclear whether Mtus1 ablation is directly related to cardiac hypertrophy. Moreover, the authors did not clarify which variants affected those phenotypes. In this study, using cardiac-specific Mtus1A TG mice, we showed that the Mtus1A variant is directly related to cardiac hypertrophy. Furthermore, we showed that Mtus1A directly suppresses cardiomyocyte hypertrophy through ERK signaling reduction. Therefore, the present study can be regarded as the first report elucidating the pathophysiological role of Mtus1A in the heart.

Cardiac-specific ERK2 deletion mice exhibited a reduced hypertrophic response to pressure overload and deterioration of LV function.[36] These findings are consistent with our data in Mtus1A TG mice. Consistent with the result in ERK2 knockout mice, the heart-to-body-weight ratio tended to be higher in Mtus1A TG mice after TAC; however, there was no statistically significant difference in the heart to body weight ratio between these and WT mice.

Here we showed that Mtus1A overexpression attenuates cardiac hypertrophy and adversely affects cardiac function. It is believed that there are 2 aspects to cardiac hypertrophy: adaptive and maladaptive phases.[37–39] Adaptive cardiac hypertrophy represents a physiological response to increased

workloads, which enables an increase in cardiac contractility. However, prolonged and excessive hypertrophy leads to a maladaptive phase, resulting in heart failure. TAC-induced cardiac hypertrophy is an adaptive response to pressure overload.[40] Mtus1A activation may inhibit adaptive hypertrophy, since we observed that Mtus1A overexpression reduced both cardiac hypertrophy and function. Thus, further investigation into the nature of cardiomyocytes with and without Mtus1A activation may reveal differences between adaptive and maladaptive cardiac hypertrophy.

We performed genome-wide exon-level analysis and identified the Mtus1A variant as a novel regulator of cardiac hypertrophy. Elucidation of the splicing mechanism of *Mtus1* could aid the development of novel treatments for cardiac hypertrophy.

Acknowledgments

We thank Akiko Ogai for technical assistance; Dr Naoto Minamino for assistance with Mtus1 antibody production. We are grateful to Dr Jeffrey Robbins for the gift of murine α-MHC promoter expression plasmid.

Sources of Funding

This work was supported by Grants-in-aid from the Ministry of Health, Labour and Welfare, Japan (H23-Nanchi-Ippan-22 to Kitakaze); Grants-in-aid from the Ministry of Education, Culture, Sports, Science and Technology, Japan (21590945 to Asakura); research grants from Mochida Memorial Foundation for Medical and Pharmaceutical Research (Asakura); SENSHIN Medical Research Foundation (Asakura); and Medical Research Encouragement Prize of The Japan Medical Association (Asakura).

Disclosures

None.

References

1. Rabkin SW, Goutsouliak V, Kong JY. Angiotensin II induces activation of phosphatidylinositol 3-kinase in cardiomyocytes. *J Hypertens*. 1997;15:891–899.
2. Schluter KD, Simm A, Schafer M, Taimor G, Piper HM. Early response kinase and PI 3-kinase activation in adult cardiomyocytes and their role in hypertrophy. *Am J Physiol*. 1999;276:H1655–H1663.
3. Crackower MA, Oudit GY, Kozieradzki I, Sarao R, Sun H, Sasaki T, Hirsch E, Suzuki A, Shioi T, Irie-Sasaki J, Sah R, Cheng HY, Rybin VO, Lembo G, Fratta L, Oliveira-dos-Santos AJ, Benovic JL, Kahn CR, Izumo S, Steinberg SF, Wymann MP, Backx PH, Penninger JM. Regulation of myocardial contractility and cell size by distinct PI3K-PTEN signaling pathways. *Cell*. 2002;110:737–749.
4. Ni YG, Berenji K, Wang N, Oh M, Sachan N, Dey A, Cheng J, Lu G, Morris DJ, Castrillon DH, Gerard RD, Rothermel BA, Hill JA. Foxo transcription factors blunt cardiac hypertrophy by inhibiting calcineurin signaling. *Circulation*. 2006;114:1159–1168.
5. Li HH, Kedar V, Zhang C, McDonough H, Arya R, Wang DZ, Patterson C. Atrogin-1/muscle atrophy F-box inhibits calcineurin-dependent cardiac hypertrophy by participating in an SCF ubiquitin ligase complex. *J Clin Invest*. 2004;114:1058–1071.
6. Bueno OF, De Windt LJ, Tymitz KM, Witt SA, Kimball TR, Klevitsky R, Hewett TE, Jones SP, Lefer DJ, Peng CF, Kitsis RN, Molkentin JD. The MEK1-ERK1/2 signaling pathway promotes compensated cardiac hypertrophy in transgenic mice. *EMBO J*. 2000;19:6341–6350.
7. Yussman MG, Toyokawa T, Odley A, Lynch RA, Wu G, Colbert MC, Aronow BJ, Lorenz JN, Dorn GW II. Mitochondrial death protein nix is induced in cardiac hypertrophy and triggers apoptotic cardiomyopathy. *Nat Med*. 2002;8:725–730.
8. Strom CC, Aplin M, Ploug T, Christoffersen TE, Langfort J, Viese M, Galbo H, Haunso S, Sheikh SP. Expression profiling reveals differences in metabolic gene expression between exercise-induced cardiac effects and maladaptive cardiac hypertrophy. *FEBS J*. 2005;272:2684–2695.
9. Sharma UC, Pokharel S, van Brakel TJ, van Berlo JH, Cleutjens JP, Schroen B, Andre S, Crijns HJ, Gabius HJ, Maessen J, Pinto YM. Galectin-3 marks activated macrophages in failure-prone hypertrophied hearts and contributes to cardiac dysfunction. *Circulation*. 2004;110:3121–3128.
10. Clark TA, Schweitzer AC, Chen TX, Staples MK, Lu G, Wang H, Williams A, Blume JE. Discovery of tissue-specific exons using comprehensive human exon microarrays. *Genome Biol*. 2007;8:R64.
11. Johnson JM, Castle J, Garrett-Engele P, Kan Z, Loerch PM, Armour CD, Santos R, Schadt EE, Stoughton R, Shoemaker DD. Genome-wide survey of human alternative pre-mRNA splicing with exon junction microarrays. *Science*. 2003;302:2141–2144.
12. Pan Q, Shai O, Lee LJ, Frey BJ, Blencowe BJ. Deep surveying of alternative splicing complexity in the human transcriptome by high-throughput sequencing. *Nat Genet*. 2008;40:1413–1415.
13. Wang ET, Sandberg R, Luo S, Khrebtukova I, Zhang L, Mayr C, Kingsmore SF, Schroth GP, Burge CB. Alternative isoform regulation in human tissue transcriptomes. *Nature*. 2008;456:470–476.
14. Park JY, Li W, Zheng D, Zhai P, Zhao Y, Matsuda T, Vatner SF, Sadoshima J, Tian B. Comparative analysis of mRNA isoform expression in cardiac hypertrophy and development reveals multiple post-transcriptional regulatory modules. *PLoS One*. 2011;6:e22391.
15. Kim T, Kim JO, Oh JG, Hong SE, Kim do H. Pressure-overload cardiac hypertrophy is associated with distinct alternative splicing due to altered expression of splicing factors. *Mol Cells*. 2014;37:81–87.
16. Kong SW, Hu YW, Ho JW, Ikeda S, Polster S, John R, Hall JL, Bisping E, Pieske B, dos Remedios CG, Pu WT. Heart failure-associated changes in RNA splicing of sarcomere genes. *Circ Cardiovasc Genet*. 2010;3:138–146.
17. Seibold S, Rudroff C, Weber M, Galle J, Wanner C, Marx M. Identification of a new tumor suppressor gene located at chromosome 8p21.3-22. *FASEB J*. 2003;17:1180–1182.
18. Wruck CJ, Funke-Kaiser H, Pufe T, Kusserow H, Menk M, Schefe JH, Kruse ML, Stoll M, Unger T. Regulation of transport of the angiotensin AT2 receptor by a novel membrane-associated Golgi protein. *Arterioscler Thromb Vasc Biol*. 2005;25:57–64.
19. Nouet S, Amzallag N, Li JM, Louis S, Seitz I, Cui TX, Alleaume AM, Di Benedetto M, Boden C, Masson M, Strosberg AD, Horiuchi M, Couraud PO, Nahmias C. Trans-inactivation of receptor tyrosine kinases by novel angiotensin II AT2 receptor-interacting protein, ATIP. *J Biol Chem*. 2004;279:28989–28997.
20. Ding X, Zhang N, Cai Y, Li S, Zheng C, Jin Y, Yu T, Wang A, Zhou X. Down-regulation of tumor suppressor MTUS1/ATIP is associated with enhanced proliferation, poor differentiation and poor prognosis in oral tongue squamous cell carcinoma. *Mol Oncol*. 2012;6:73–80.
21. Liao Y, Ishikura F, Beppu S, Asakura M, Takashima S, Asanuma H, Sanada S, Kim J, Ogita H, Kuzuya T, Node K, Kitakaze M, Hori M. Echocardiographic assessment of LV hypertrophy and function in aortic-banded mice: necropsy validation. *Am J Physiol Heart Circ Physiol*. 2002;282:H1703–H1708.
22. Sasaki H, Asanuma H, Fujita M, Takahama H, Wakeno M, Ito S, Ogai A, Asakura M, Kim J, Minamino T, Takashima S, Sanada S, Sugimachi M, Komamura K, Mochizuki N, Kitakaze M. Metformin prevents progression of heart failure in dogs: role of AMP-activated protein kinase. *Circulation*. 2009;119:2568–2577.
23. Sawyer DB, Siwik DA, Xiao L, Pimentel DR, Singh K, Colucci WS. Role of oxidative stress in myocardial hypertrophy and failure. *J Mol Cell Cardiol*. 2002;34:379–388.
24. Sundaresan NR, Gupta M, Kim G, Rajamohan SB, Isbatan A, Gupta MP. Sirt3 blocks the cardiac hypertrophic response by augmenting Foxo3a-dependent antioxidant defense mechanisms in mice. *J Clin Invest*. 2009;119:2758–2771.

25. Di Benedetto M, Pineau P, Nouet S, Berhouet S, Seitz I, Louis S, Dejean A, Couraud PO, Strosberg AD, Stoppa-Lyonnet D, Nahmias C. Mutation analysis of the 8p22 candidate tumor suppressor gene ATIP/MTUS1 in hepatocellular carcinoma. *Mol Cell Endocrinol*. 2006;252:207–215.
26. Zuern C, Heimrich J, Kaufmann R, Richter KK, Settmacher U, Wanner C, Galle J, Seibold S. Down-regulation of MTUS1 in human colon tumors. *Oncol Rep*. 2010;23:183–189.
27. Zhao T, Ding X, Chang B, Zhou X, Wang A. MTUS1/ATIP3a down-regulation is associated with enhanced migration, invasion and poor prognosis in salivary adenoid cystic carcinoma. *BMC Cancer*. 2015;15:203.
28. Fujita T, Mogi M, Min LJ, Iwanami J, Tsukuda K, Sakata A, Okayama H, Iwai M, Nahmias C, Higaki J, Horiuchi M. Attenuation of cuff-induced neointimal formation by overexpression of angiotensin II type 2 receptor-interacting protein 1. *Hypertension*. 2009;53:688–693.
29. Michelakis ED. Mitochondrial medicine: a new era in medicine opens new windows and brings new challenges. *Circulation*. 2008;117:2431–2434.
30. Dai DF, Johnson SC, Villarin JJ, Chin MT, Nieves-Cintron M, Chen T, Marcinek DJ, Dorn GW II, Kang YJ, Prolla TA, Santana LF, Rabinovitch PS. Mitochondrial oxidative stress mediates angiotensin II-induced cardiac hypertrophy and Galphaq overexpression-induced heart failure. *Circ Res*. 2011;108:837–846.
31. Amin JK, Xiao L, Pimental DR, Pagano PJ, Singh K, Sawyer DB, Colucci WS. Reactive oxygen species mediate alpha-adrenergic receptor-stimulated hypertrophy in adult rat ventricular myocytes. *J Mol Cell Cardiol*. 2001;33:131–139.
32. Dai DF, Hsieh EJ, Liu Y, Chen T, Beyer RP, Chin MT, MacCoss MJ, Rabinovitch PS. Mitochondrial proteome remodelling in pressure overload-induced heart failure: the role of mitochondrial oxidative stress. *Cardiovasc Res*. 2012;93:79–88.
33. Song Y, Xu J, Li Y, Jia C, Ma X, Zhang L, Xie X, Zhang Y, Gao X, Zhang Y, Zhu D. Cardiac ankyrin repeat protein attenuates cardiac hypertrophy by inhibition of ERK1/2 and TGF-beta signaling pathways. *PLoS One*. 2012;7:e50436.
34. Rachmin I, Tshori S, Smith Y, Oppenheim A, Marchetto S, Kay G, Foo RS, Dagan N, Golomb E, Gilon D, Borg JP, Razin E. Erbin is a negative modulator of cardiac hypertrophy. *Proc Natl Acad Sci USA*. 2014;111:5902–5907.
35. Zuern C, Krenacs L, Starke S, Heimrich J, Palmetshofer A, Holtmann B, Sendtner M, Fischer T, Galle J, Wanner C, Seibold S. Microtubule associated tumor suppressor 1 deficient mice develop spontaneous heart hypertrophy and SLE-like lymphoproliferative disease. *Int J Oncol*. 2012;40:1079–1088.
36. Ulm S, Liu W, Zi M, Tsui H, Chowdhury SK, Endo S, Satoh Y, Prehar S, Wang R, Cartwright EJ, Wang X. Targeted deletion of ERK2 in cardiomyocytes attenuates hypertrophic response but provokes pathological stress induced cardiac dysfunction. *J Mol Cell Cardiol*. 2014;72:104–116.
37. Wikman-Coffelt J, Parmley WW, Mason DT. The cardiac hypertrophy process. Analyses of factors determining pathological vs. physiological development. *Circ Res*. 1979;45:697–707.
38. Frey N, Katus HA, Olson EN, Hill JA. Hypertrophy of the heart: a new therapeutic target? *Circulation*. 2004;109:1580–1589.
39. Sakamoto M, Minamino T, Toko H, Kayama Y, Zou Y, Sano M, Takaki E, Aoyagi T, Tojo K, Tajima N, Nakai A, Aburatani H, Komuro I. Upregulation of heat shock transcription factor 1 plays a critical role in adaptive cardiac hypertrophy. *Circ Res*. 2006;99:1411–1418.
40. Sano M, Minamino T, Toko H, Miyauchi H, Orimo M, Qin Y, Akazawa H, Tateno K, Kayama Y, Harada M, Shimizu I, Asahara T, Hamada H, Tomita S, Molkentin JD, Zou Y, Komuro I. p53-induced inhibition of Hif-1 causes cardiac dysfunction during pressure overload. *Nature*. 2007;446:444–448.

JAHA/2016/003521-T2

SUPPLEMENTAL MATERIAL

Identification of the Mtus1 Splice Variant as a Novel Inhibitory Factor against Cardiac Hypertrophy

Shin Ito, MD; Masanori Asakura, MD, PhD; Yulin Liao, MD, PhD; Kyung-Duk Min, MD, PhD; Ayako Takahashi, MD, PhD; Kazuhiro Shindo, MD; Satoru Yamazaki, PhD; Osamu Tsukamoto, MD, PhD; Hiroshi Asanuma, MD, PhD; Masaki Mogi, MD, PhD; Masatsugu Horiuchi, MD, PhD; Yoshihiro Asano, MD, PhD; Shoji Sanada, MD, PhD; Tetsuo Minamino, MD, PhD; Seiji Takashima, MD, PhD; Naoki Mochizuki, MD, PhD; and Masafumi Kitakaze, MD, PhD

Departments of Cell Biology (S.I., KD.M., A.T., K.S., S.Y., N.M.) and Clinical Research and Development (M.A., M.K.), National Cerebral and Cardiovascular Center, Osaka, Japan; Department of Cardiology (Y.L.), Nanfang Hospital, Southern Medical University, Guangzhou, China; Department of Cardiovascular Medicine (H.A.), Kyoto Prefectural University of Medicine, Kyoto, Japan; Department of Molecular Cardiovascular Biology and Pharmacology (M.M., M.H.), Ehime University, Graduate School of Medicine, Ehime, Japan; Departments of Medical Biochemistry (O. T., S.T.) and Cardiovascular Medicine (S.S., Y.A., T.M.), Osaka University Graduate School of Medicine, Osaka, Japan.

Table S1. Physiological Findings and Cardiac Parameters Obtained by Either Echocardiography or Cardiac Catheterization

	Sham 8 wks (n = 4)	TAC 8 wks (n = 4)
Physiological Findings		
BW, g	26.6 ± 1.3	25.3 ± 2.6
HW, mg	111.0 ± 9.1	275.3 ± 15.8**
LW, mg	165.3 ± 26.8	417.8 ± 126.2**
HW/BW, mg/g	4.2 ± 0.2	11.0 ± 1.3**
LW/BW, mg/g	6.2 ± 0.8	17.0 ± 6.6*
Echocardiographic Findings		
LVEDD, mm	2.95 ± 0.28	4.57 ± 0.8**
LVESD, mm	1.34 ± 0.39	3.81 ± 0.10**
FS, %	55.2 ± 8.7	17.4 ± 7.7**
LVPWT, mm	0.67 ± 0.03	0.79 ± 0.18
Catheterization Findings		
HR, bpm	526 ± 73	351 ± 97*
LVSP, mmHg	108.2 ± 13.8	183.3 ± 44.1*
LVEDP, mmHg	1.4 ± 3.3	25.2 ± 3.1**
dP/dt max, mmHg/s	12953 ± 2967	6114 ± 2887*
dP/dt min, mmHg/s	−10920 ± 2982	−5183 ± 2659*
τ, ms	7.91 ± 1.50	24.48 ± 12.41

Fractional shortening (FS) was calculated as (LVEDD−LVESD)/LVEDD ×100. The dP/dt max and dP/dt min represent the maximum rates of pressure development during contraction and relaxation, respectively. τ, time constant of isovolumic relaxation. TAC, transverse aortic constriction; BW, body weight; HW, heart weight; LW, lung weight; LVEDD, left ventricular end-diastolic dimension; LVESD, left ventricular end-systolic dimension; LVPWT, left ventricular posterior wall thickness; HR, heart rate; LVSP, systolic pressure; LVEDP,

end-diastolic pressure. Data are shown as mean ± SD. *$P < 0.05$, **$P < 0.01$ versus sham.

Table S2. Genes (46) with Changes in the Splicing Pattern but no Changes in the Gene Expression Levels

RefSeq ID	Gene Symbol	Splicing Analysis				Gene-Level Analysis	
		Probe Set ID	Exon ID	FC	*P* Value	FC	*P* Value
NM_133979	*Ano10*	5532018	880320	−8.22	0.0000	1.00	0.9804
		5505745	880320	−5.80	0.0001		
NM_175476	*Arhgap25*	4919141	721099	2.47	0.0011	1.02	0.9425
NM_028266	*Col16a1*	4747533	589806	2.87	0.0004	−1.01	0.9451
		4341030	589803	2.60	0.0007		
		5425761	589885	2.58	0.0009		
		4305229	589805	2.06	0.0007		
NM_025311	*D14Ertd449e*	5333391	264577	−2.69	0.0013	−1.02	0.6119
NM_016974	*Dbp*	5224636	739841	2.32	0.0289	−1.01	0.9588
NM_007883	*Dsg2*	5075759	390151	2.35	0.0130	1.03	0.7788
NM_181594	*Edc4*	4885056	805016	−2.03	0.0320	−1.00	0.9670
NM_013813	*Epb41l3*	5169699	364432	2.37	0.0096	−1.00	0.9975
		4799509	364456	2.29	0.0276		
		5000482	364446	2.08	0.0415		

NM_010269	*Gdap2*	5145896	532450	−2.42	0.0227	−1.01	0.9037
NM_054102	*Ivns1abp*	5084153	22515	−2.21	0.0037	1.01	0.7504
NM_027696	*Mier1*	4393355	583621	2.25	0.0065	1.00	0.9855
NM_001005863	*Mtus1*	5023875	816914	−2.49	0.0020	1.04	0.1274
		4736902	816922	−2.24	0.0044		
		5509738	816910	2.22	0.0040		
		5473544	816924	−2.15	0.0012		
		4584003	816924	−2.07	0.0071		
		5247471	816924	−2.00	0.0036		
NM_183426	*Sbno2*	5378892	98576	2.18	0.0011	−1.01	0.9798
NM_011355	*Sfpi1*	5148804	460287	2.61	0.0308	1.08	0.6707
NM_178869	*Ttll1*	5053948	313197	−3.04	0.0104	−1.18	0.5304
		4782753	313196	−2.56	0.0173		
		4479800	313196	−2.27	0.0493		
NM_144873	*Uhrf2*	5339605	424323	−2.52	0.0175	1.00	0.9912
NM_054041	*Antxr1*	5240805	720999	−2.61	0.0040	1.02	0.8615
NM_009685	*Apbb1*	5486110	775346	2.12	0.0037	1.01	0.9201

NM_028176	*Cda*	4777112	619931	−2.73	0.0019	1.10	0.3465
		4841419	619930	−2.31	0.0016		
NM_177381	*Cog3*	5490318	274739	−2.27	0.0010	1.00	0.9950
NM_031163	*Col2a1*	5387581	316592	2.50	0.0168	1.00	0.9993
		4588907	316585	2.26	0.0068		
NM_199473	*Col8a2*	4546188	588720	3.37	0.0086	−1.01	0.9102
		4786438	588720	3.04	0.0073		
NM_009953	*Crhr2*	5214517	716824	2.01	0.0046	−1.00	0.9924
NM_133710	*Ctdspl*	5186053	855776	2.31	0.0023	−1.01	0.9532
NM_021281	*Ctss*	4869518	531408	−2.24	0.0101	1.02	0.7580
NM_021474	*Efemp2*	5569004	419066	−2.27	0.0280	−1.01	0.8889
		5094998	419067	−2.07	0.0337		
NM_010494	*Icam2*	5079407	158011	−2.37	0.0114	1.01	0.8664
NM_175641	*Ltbp4*	4886208	761211	−2.23	0.0013	−1.00	0.9458
NM_008610	*Mmp2*	4424025	802648	−2.26	0.0004	−1.01	0.8996
NM_177167	*Ppm1e*	5205442	152532	−2.15	0.0410	1.00	0.9819
NM_199447	*Rrp12*	4630666	439492	−2.18	0.0017	1.00	0.9988

		4566479	439477	−2.05	0.0061		
NM_024225	*Snx5*	5161738	506079	−2.32	0.0130	1.02	0.7396
NM_029688	*Srxn1*	4953126	471659	2.09	0.0216	−1.04	0.7321
NM_031402	*Crispld1*	4945515	1944	2.13	0.0007	1.00	0.9841
NM_010206	*Fgfr1*	5333109	791135	−2.56	0.0027	1.01	0.9494
NM_010220	*Fkbp5*	5394790	373898	−2.50	0.0292	1.02	0.8949
NM_010580	*Itgb5*	4581508	325576	−2.09	0.0006	1.00	0.9230
NM_177784	*Klhl23*	5235871	456681	2.01	0.0001	1.01	0.9688
NM_173379	*Leprel1*	4513573	339573	−2.24	0.0171	1.04	0.8728
NM_175260	*Myh10*	4893000	120355	−2.27	0.0003	1.00	0.9793
NM_022410	*Myh9*	4862001	311414	−2.39	0.0190	1.00	0.9988
		4362366	311431	−2.05	0.0439		
NM_008787	*Pcnt*	4775454	97630	2.09	0.0161	−1.00	0.9927
NM_008861	*Pkd2*	4997957	643838	−2.16	0.0006	1.00	0.9860
NM_009161	*Sgca*	4363794	154078	−2.05	0.0003	1.00	0.8832
NM_011774	*Slc30a4*	4877721	501718	−2.15	0.0122	1.00	0.9695
NM_027641	*Spef1*	4788900	503865	3.62	0.0007	−1.02	0.5314

FC, fold change.

Table S3. Physiological and Echocardiographic Findings Data of Wild-Type (WT) and Mitochondrial Tumor Suppressor 1 (Mtus1) A Transgenic (TG) Mice induced by Transverse Aortic Constriction (TAC)

	WT sham (n = 3)	**Mtus1A TG sham (n = 3)**	**WT TAC (n = 6)**	**Mtus1A TG TAC (n = 4)**
SBP, mmHg	102 ± 4	100 ± 2	92 ± 5*	87 ± 5††
DBP, mmHg	64 ± 2	60 ± 3	54 ± 7	52 ± 7
HR, bpm	632 ± 29	614 ± 30	521 ± 87	379 ± 12††§
BW, g	25.3 ± 1.5	26.0 ± 1.5	25.2 ± 1.7	24.1 ± 2.1
HW/BW, mg/g	5.84 ± 0.26	5.19 ± 0.28*	9.68 ± 0.85**	10.14 ± 1.60††
LW/BW, mg/g	6.02 ± 0.07	6.13 ± 0.10	7.62 ± 2.13	15.33 ± 5.60†§
LVEDD, mm	3.14 ± 0.09	3.46 ± 0.07**	4.12 ± 0.25**	5.63 ± 0.25††§§
LVESD, mm	1.53 ± 0.05	2.09 ± 0.19**	3.01 ± 0.24**	4.99 ± 0.34††§§
FS, %	51.4 ± 1.2	39.6 ± 4.5**	27.1 ± 4.5**	11.4 ± 2.7††§§
LVPWT, mm	0.70 ± 0.01	0.64 ± 0.01**	0.81 ± 0.03**	0.67 ± 0.02§§

Fractional shortening (FS) was calculated as (LVEDD−LVESD)/LVEDD ×100. SBP, systolic blood pressure; DBP, diastolic blood pressure; HR, heart rate; HW, heart weight; BW, body weight; LW, lung weight; LVEDD, left ventricular end-diastolic dimension; LVESD, left ventricular end-systolic dimension; LVPWT, left ventricular posterior wall thickness. Data are shown as mean ± SD. **P < 0.05, **P < 0.01 versus WT-sham; $^{\dagger}P$ < 0.05, $^{\dagger\dagger}P$ < 0.01 versus Mtus1A TG-sham; $^{\S}P$ < 0.05, $^{\S\S}P$ < 0.01 versus WT-TAC.

Figure S1

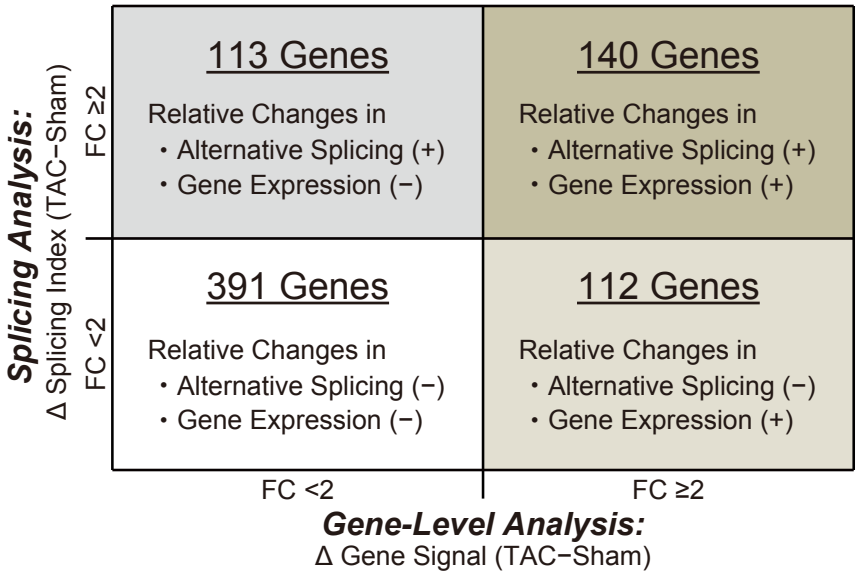
113 Genes
Relative Changes in
• Alternative Splicing (+)
• Gene Expression (−)
140 Genes
Relative Changes in
• Alternative Splicing (+)
• Gene Expression (+)
391 Genes
Relative Changes in
• Alternative Splicing (−)
• Gene Expression (−)
112 Genes
Relative Changes in
• Alternative Splicing (−)
• Gene Expression (+)
Splicing Analysis:
Δ Splicing Index (TAC−Sham)
FC ≥2
FC <2
FC <2
FC ≥2
Gene-Level Analysis:
Δ Gene Signal (TAC−Sham)

Figure S2

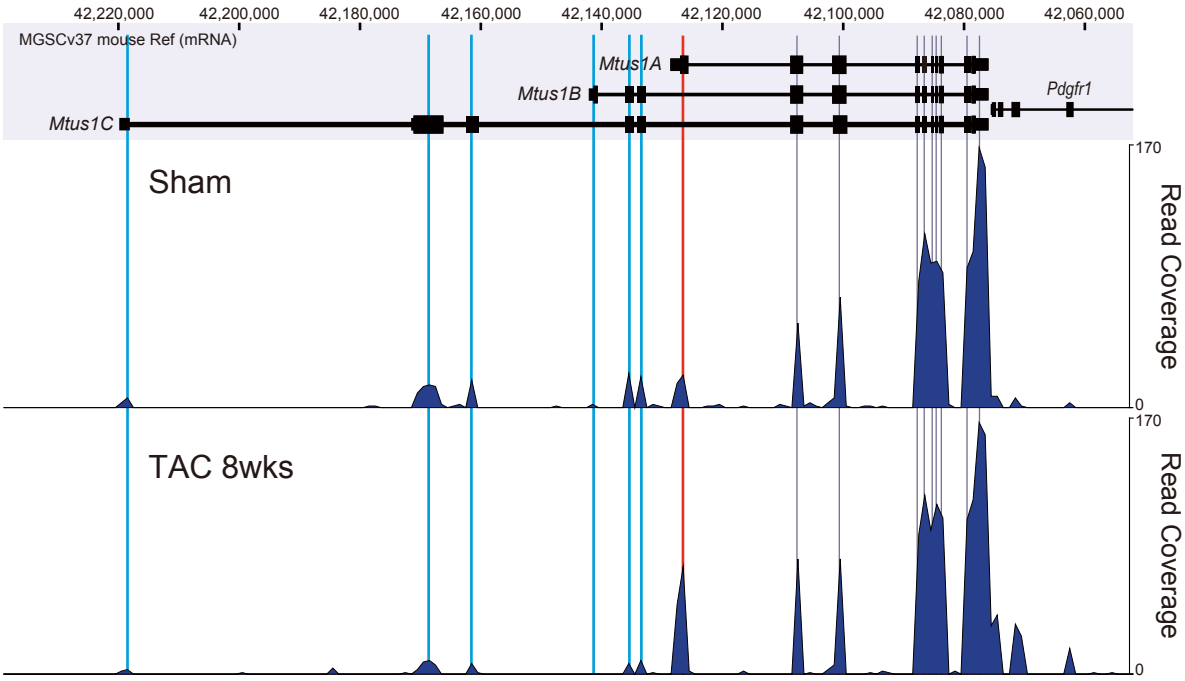
42,220,000
42,200,000
42,180,000
42,160,000
42,140,000
42,120,000
42,100,000
42,080,000
42,060,000
MGSCv37 mouse Ref (mRNA)
Mtus1A
Mtus1B
Mtus1C
Pdgfr1
Sham
170
Read Coverage
0
TAC 8wks
170
Read Coverage
0

Figure S3

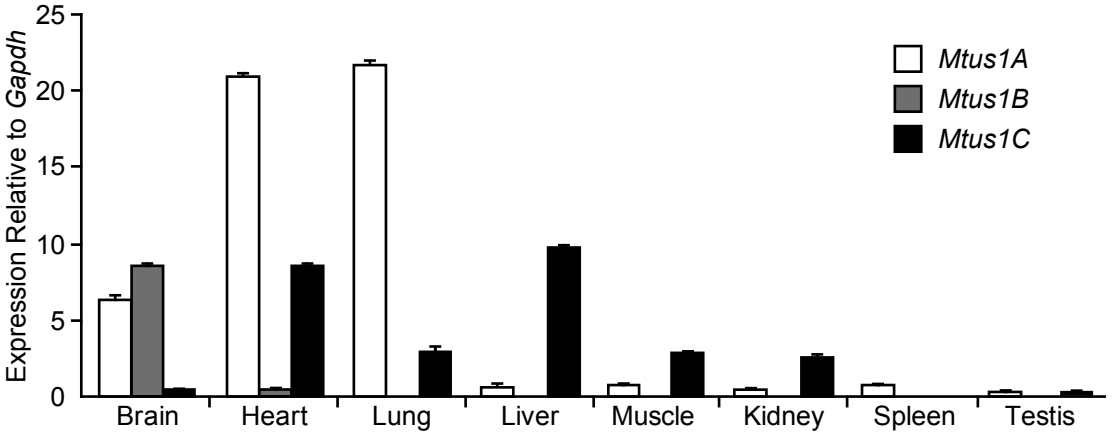
Expression Relative to Gapdh
25
20
15
10
5
0
Mtus1A
Mtus1B
Mtus1C
Brain
Heart
Lung
Liver
Muscle
Kidney
Spleen
Testis

Figure S4

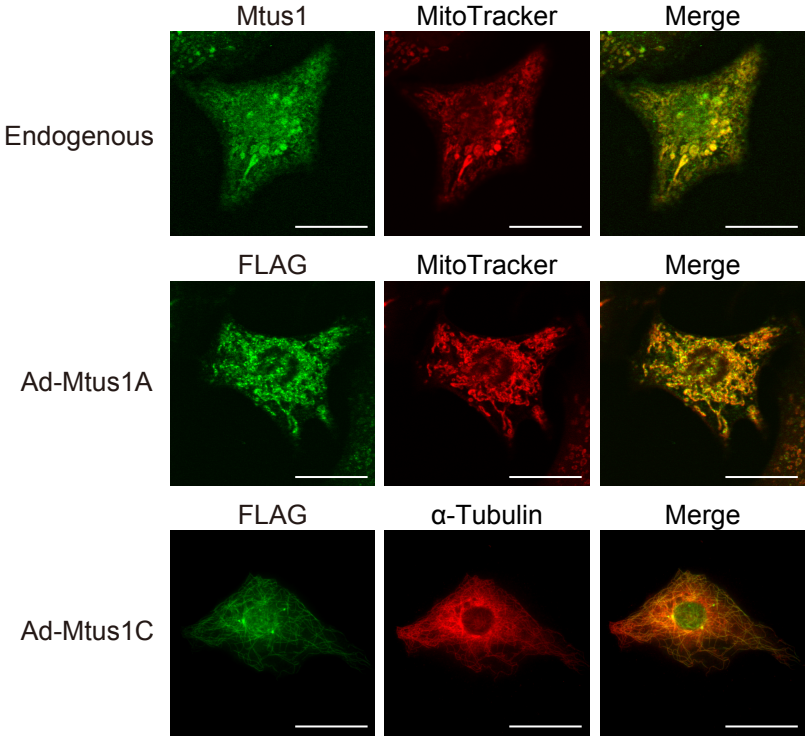
Mtus1
MitoTracker
Merge
Endogenous
FLAG
MitoTracker
Merge
Ad-Mtus1A
FLAG
α-Tubulin
Merge
Ad-Mtus1C

Figure S5

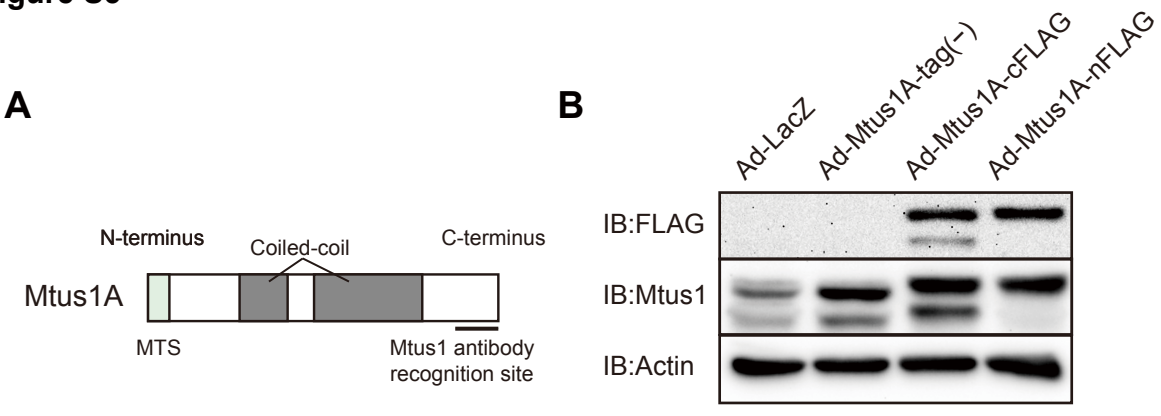
A
N-terminus
Coiled-coil
C-terminus
Mtus1A
MTS
Mtus1 antibody
recognition site
B
Ad-LacZ
Ad-Mtus1A-tag(−)
Ad-Mtus1A-cFLAG
Ad-Mtus1A-nFLAG
IB:FLAG
IB:Mtus1
IB:Actin

Figure S6

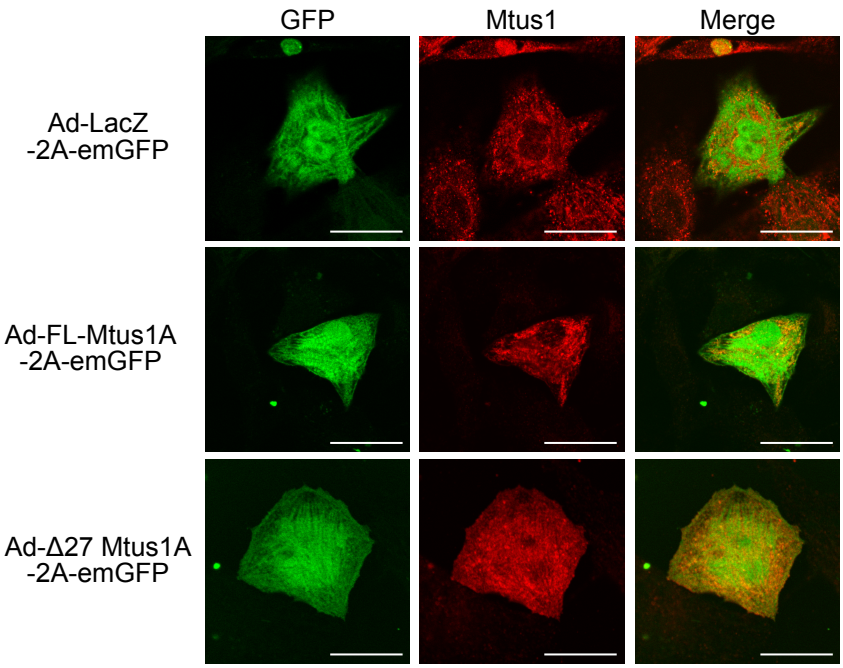
GFP
Mtus1
Merge
Ad-LacZ
-2A-emGFP
Ad-FL-Mtus1A
-2A-emGFP
Ad-Δ27 Mtus1A
-2A-emGFP

Figure S7

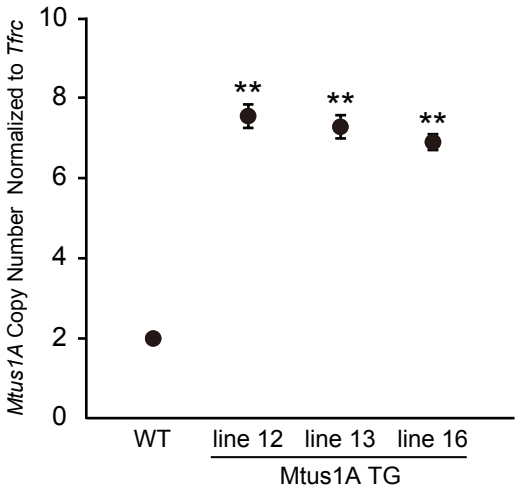
10
8
6
4
2
0
Mtus1A Copy Number Normalized to Tfrc
**
**
**
WT
line 12
line 13
line 16
Mtus1A TG

Supplemental Figure Legends

Figure S1.

Classification of genes identified by gene-level or splicing analysis. The upper left rectangle indicates 113 genes that demonstrated changes in splicing pattern (splicing index ≥2, $P < 0.05$) but without changes in gene expression level; the lower right rectangle indicates 112 genes with changes in gene expression level (fold change ≥2, $P < 0.05$) but without changes in splicing pattern; the upper right rectangle indicates 140 genes with changes in gene expression level and splicing pattern; and the lower left rectangle indicates 391 genes without change in expression level or splicing pattern. TAC, transverse aortic constriction; FC, fold change.

Figure S2.

Differences in the exon expression pattern of *Mtus1* by RNA-Seq. The sequenced reads were mapped to the reference mouse genome (MGSCv37). Blue and red vertical lines show the decreased and increased number of reads mapped to the annotated exons in the transverse aortic constriction (TAC) hearts compared with that in the sham operation hearts. Black vertical lines show the unchanged number of reads in the TAC hearts.

Figure S3.

Tissue distribution of *Mtus1* variants. Real-time PCR was performed with a mouse multiple tissue cDNA panel (Clontech) using variant-specific TaqMan probes and primers. Data are shown as mean ± SD (n = 2 in each).

Figure S4.

Subcellular localization of mitochondrial tumor suppressor 1 (Mtus1) variants in cardiomyocytes. The upper images indicate the localization of endogenous Mtus1 variants (green) and mitochondria (red); the middle images indicate the localization of FLAG-Mtus1A (green) and mitochondria (red); and the lower images indicate the localization of

FLAG-Mtus1C (green) and microtubule (red). Endogenous Mtus1 variants were stained with anti-Mtus1 antibody. Mitochondria and microtubules were stained with MitoTracker Red and anti-α-Tubulin antibody, respectively. Two images were merged to produce a third image. Neonatal rat cardiomyocytes were infected with adenoviruses expressing C-terminal FLAG-tagged Mtus1A or N-terminal FLAG-tagged Mtus1C for 48 h and then stained with anti-FLAG antibody. Images were visualized using a FLUOVIEW FV10i confocal microscope (scale bar: 30 μm).

Figure S5.

A, The domain structure of mitochondrial tumor suppressor 1 (*Mtus1*) A. An Mtus1 polyclonal antibody was designed to recognize an epitope in the C-terminal region. **B,** Neonatal rat cardiomyocytes were infected with Ad-LacZ or Ad-Mtus1A (non-tag, C-terminus FLAG tag, and N-terminus FLAG tag) for 48 h. The cell lysates were immunoblotted with antibodies against FLAG, Mtus1, and Actin. MTS, mitochondrial targeting sequence.

Figure S6.

Immunofluorescent staining of neonatal rat cardiomyocytes, overexpressing Ad-LacZ-2A-emGFP, Ad-full length (FL)-Mtus1A-2A-emGFP, or Ad-Δ27 Mtus1A-2A-emGFP for 48 h. The images on the left indicate GFP expression in the cytosol using 2A self-cleaving peptides. The images in the middle indicate Mtus1A expression in cardiomyocytes stained with anti-Mtus1 antibody (red). Two images were merged to produce a third image. Images were visualized using a FLUOVIEW FV10i confocal microscope (scale bar: 30 μm).

Figure S7.

Transgene copy number in cardiac-specific mitochondrial tumor suppressor 1A (Mtus1A) transgenic (TG) mice compared with that in wild type (WT) mice. The genomic DNA from three lines of TG mice were analyzed by real-time PCR-based copy number assay (line 12, n = 3; line 13, n = 4; line 16, n = 4; and WT, n = 5). All data were normalized to *Tfrc*. Data are

shown as mean ± SD. **$P < 0.01$ versus the WT mice.

Video S1.

Echocardiography of a wild type (WT) mouse at 4 weeks after sham operation.

Video S2.

Echocardiography of a mitochondrial tumor suppressor 1 A (Mtus1A) transgenic (TG) mouse at 4 weeks after sham operation.

Video S3.

Echocardiography of a wild type (WT) mouse at 4 weeks after transverse aortic constriction (TAC).

Video S4.

Echocardiography of a mitochondrial tumor suppressor 1A (Mtus1A) transgenic (TG) mouse at 4 weeks after transverse aortic constriction (TAC).